STUDY OF HYDROGEN ASSISTED CRACKING IN SHIP BUILDING GRADE STEEL

A Thesis Submitted in Partial Fulfillment of Requirement for the Degree of

Master of Technology

In

Mechanical Engineering

[Specialization: Steel Technology]

Submitted By

Pawan Kumar Sahu

Roll No.212MM2461

Department of Metallurgy and Material Engineering

National Institute of Technology

Rourkela-769008

May2014

STUDY OF HYDROGEN ASSISTED CRACKING IN SHIP BUILDING GRADE STEEL

A Thesis Submitted in Partial Fulfillment of Requirement for the Degree of

Master of Technology

In

Mechanical Engineering

[Specialization: Steel Technology]

Submitted

By

Pawan Kumar Sahu

Roll No.212MM2461

Under The Guidance of

Prof A.Basu

And

Dr. S. Sivaprasad (CSIR, NML)

Department of Metallurgy and Material Engineering

National Institute of Technology

Rourkela-769008

May2014

National Institute Of Technology Rourkela

CERTIFICATES

This is to certify that the thesis entitled, **"STUDY OF HYDROGEN ASSISTED CRACKING ON SHIP BUILDING GRADE STEEL" "**submitted by **MR. PAWAN KUMAR SAHU**, in fulfillment of the requirements for the of master of technology degree in "**MECHANICAL ENGINEERING (Specialization: Steel Technology) AT THE NATIONAL INSTITUTE OF TECHNOLOGY ROURKELA"** is an authentic work carried out by him under our supervision and guidance.

To the best of our knowledge, the matter embodied in the thesis has not been submitted to any other University/ Institute for the award of any degree or diploma.

During the working period Pawan Kumar Sahu was found to be hard working and sincere with learning attitude. Wish him success for his future.

Prof.A.Basu
Dept. Metallurgical and Materials Engineering
National Institute of Technology
Rourkela-769008

Dr. S. Sivaprasad
Dept. Material Science and Technology
CSIR- National Metallurgical Laboratory
Jamshedpur-831007

ACKNOWLEDGEMENT

With deep regards and profound respect, I take this opportunity to express my profound sense of gratitude and indebtedness to my supervisor **Prof. A. Basu**, Metallurgical and Materials Engineering Department, NIT Rourkela, for introducing the current research topic and for his inspiring supervision, constructive appreciation and valuable suggestion throughout this research work. It would have not been attainable on behalf of me to bring out this thesis without his help and constant encouragement.

I also take this opportunity to express my deep sense of gratitude to my other Supervisor **Dr. S. Sivaprasad**, (Principal Scientist, CSIR-NML, and Jamshedpur) for his excellent supervision and constant motivation throughout my course of project and helping me in all sorts of problem faced by me in my due course of stay as M.Tech. Trainee in NML, Jamshedpur**.**

I am thankful to Prof.B.C.Roy (HOD metallurgy and materials engineering NIT ROURKELA), Dr. S. Srikanth, Director, CSIR-National Metallurgical Laboratory, Jamshedpur, for providing me the opportunity to work in the research laboratory. I find great pleasure in expressing my gratitude to **Dr. H.N.BAR**. (Scientist CSIR-NML Jamshedpur), **Dr.S.Tarafdar** (HRG Head, CSIR-NML, Jamshedpur), **Mrs**. **Swapan D**.(SRF CSIR-NML Jamshedpur)**,Mr. Anindya Das**,(SRF,CSIR-NML,Jamshedpur**)** before their constant encouragement, support and valuable suggestion during the entire work period.

I also like to thank, all my group members of Mechanical property evaluation of MST Division in NML Jamshedpur, wherefrom I have got all sorts of help whenever needed, especially from **Dr. Arpan Das** (Scientist, NML, and Jamshedpur), **and Mr. Randhir Singh** (ACSIR, NML, Jamshedpur), **Mr. Ram Bhushan** (BESU Shibpur), **Mr.Alok Kumar** (NIT Durgapur)**, Mr. Awanish Mishra** (NIT Rourkela), **Mr.Prem Prakash Seth** (NIT Rourkela), **Mr.Om Prakash Tenduwe** (NIT Rourkela),**Mr. Ankit Mani Tripathi**(NIT Jamshedpur) **and Mr. Bipin Kumar Dash** (NML Jamshedpur), **Mr.Lalit Gupta** (CSIR NML), **Mr.Lallan Patro** (CSIR NML).

Thesis has been seen through to completion with the support and encouragement of numerous people including my well-wishers, my friends and colleagues. It is my pleasure to express my thanks at the end of my thesis to all those who contributed in many ways to the success of this study and made it an unforgettable experience for me.I would also appreciate the help and guidance from I learned a lot during this project and I would like to thank to each and every person who is helping me in completing this project.

Lastly but not the least, no work could have been conducted without the support of my parents and my family. They supported my endeavour for knowledge from childhood and my passion for learning owes to their encouragement.

Pawan Kumar Sahu

RollNo.212mm2461

Steel Technology

Nit Rourkela

Date

26/05/2014

CONTENTS

Title Page No

LIST OF FIGURES

List of Tables

SYMBOLS USED

V= Poisons Ratio

E= Young's Modulus

J_Q= Provisional J_{IC}Fracture Toughness

η = Coefficient In J Calculation

B= Net Specimen Thickness

b_o= Uncracked Ligament Length(w-a_o)

J_{IC}= Fracture Toughness Based on J

J= Nonlinear Fracture Toughness

ki= Stress Intensity Factor

B_e= Effective Thickness

v_{pl}= Plastic Part of The Crack Mouth Opening Displacement

σ_y = Average of Yield And Ultimate Tensile Strength

J_{total}= Total J Determine Using Area Under Load Displacement Curve

A_{pl}= Plastic Area Under Crack Mouth Opening Displacement

Δa= Crack Growth Increments

σ_y = Flow Stress

J_{pl}= Plastic Component of J

a= Crack Length

m= Plastic Constant Factor

a_p= Physical Crack Size

w= Specimen Width

a_o= Initial Crack Length

v_{el}= Elastic Displacement

J_{el}= Elastic Component of J

ABSTRACT

High strength, high toughness and good weldability are the major demanding factors for engineering structural materials uses in naval construction. HSLA-80 steel is essentially low carbon micro alloyed and copper strengthened high strength steel typically used for ship building application. The hydrogen presence in high strength steels causes untimely brittle fracture under static load condition. Hydrogen enters into metal and reduces the cohesive strength of metallic atom, creates void and enhance the brittlement. In the present study, the loss in ductility and susceptibility to fracture of HSLA80 grade steel was studied by using fracture toughness parameters (J integral and CTOD) in hydrogen and air environment. The tests were carried out with very slow displacement rate through cyclic loading. The hydrogen environment was generated with NaOH aqueous solution. Single Edge Notched Beam (SENB) samples with fatigue precrack were used for the tests. J-R and Δ-R curve were developed by ASTM standards. It is observed that fracture toughness of air environment tested sample was higher than hydrogen environment tested sample and fracture occurs after stable tearing. The fracture surface of the failed samples was examined by Scanning Electron Microscope (SEM) and it was observed that the failure occurred by cleavage, quasi cleavage and transgranular fracture. From the present study it was clear that in hydrogen environment the brittleness is more and the related fracture toughness values confirm the same. The hydrogen enhanced local plasticity is more applicable mechanism for hydrogen embrittlement. Mechanical property of the as received steel was studied by tensile testing and hardness test. Microstructural observation revealed presence of lath martensite and acicular ferrite in the steel. The experimental result obtained from the present study was found close to the models proposed earlier.

Keywords-Hydrogen embrittlement, fracture toughness, fatigue precrack,J-integral, crack tip opening displacement, crack length, monotonically load, stress intensity factor, stress ratio, resistance curve, HSLA80 steel

CHAPTER 1

INTRODUCTION

CHAPTER 1

INTRODUCTION

1.1 Background

Hydrogen damage is generic failure in many high strength steels. The effect of hydrogen on the mechanical properties of metal was first reported by Pefilin in 1926 who found the presence of hydrogen in steel caused a significant loss of ductility at room temperature under normal tensile condition [1]. Hydrogen is present everywhere, several kilometers inside the earth and above the earth. Engineering materials are unconcealed to hydrogen and they may interact with hydrogen resulting in various kinds of structural damage, hydrogen induced cracking or several loss of ductility caused by present of hydrogen in metal. Being small hydrogen can diffuse easily in metallic material and at elevated temperature the solubility and diffusivity of hydrogen increases resulting increase in chance in failure. Dissolve hydrogen reduce the cohesive strength of the metallic atoms and when these hydrogen atoms re-combine with minuscule voids in metal matrix to form hydrogen molecules, they create pressure inside the cavity leading to crack. Hydrogen damages of are two types 1.internal hydrogen assisted cracking, 2.Hydrogen environmental assisted cracking which is causes most of the damages [2]. As little as 0.0001 weight percentages of hydrogen causes cracking of steel and the fracture process in hydrogen can be intergranular, transgranular or ductile fracture depending on the stress level [3].HSLA80 is targeted to be used in some of the naval applications where hydrogen environment is pronounced. This type application need through review of fracture toughness of the steel in actual working condition. But available data related to this grade of steel is not available as scarce. In view of this the present study was targeted.

1.2 Objectives and work plan

- Characterization of HSLA80 steel by microscopy, phase identification by XRD and mechanical properties through tensile test and hardness test.
- Evaluation of fracture toughness in the elastic plastic fracture parameter of Jic and CTOD in both air and hydrogen environments and comparison
- Fracture surfaces investigation of failed mono-J tested sample in air and hydrogen environment, analysis of Type and mode of failure.

The methodology/flow sheet used in the present work is shown in Fig. 1.1.

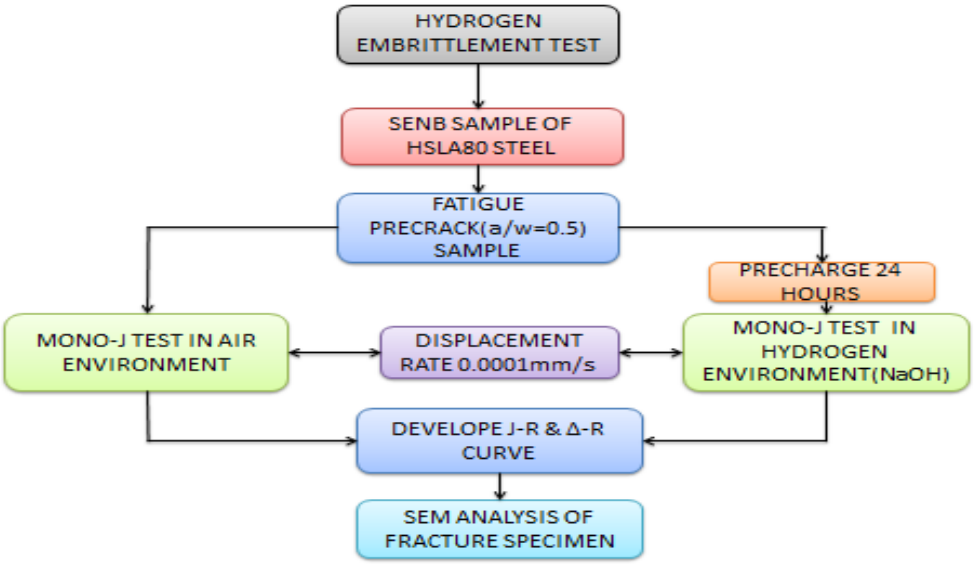

Fig. 1.1: Work plane represented by flow sheet

1.3 Scope and structure of the thesis

Many investigations have been completed to show what exact mechanism of hydrogen degradation is operative in high strength low alloy steel but till now it is like pearl search in depth of sea. Time to time many model proposed by many researcher but some time it found to be vague. In the present study of hydrogen embrittlement it will be tried to evaluate the effect of hydrogen in diluted phase (sea water) in high strength low alloy steel in slow displacement rate.

The structure of the thesis is actually in chronological order and the details are as below.

Hydrogen embrittlement mechanism, HSLA steel type and manufacturing process, microstructure, aging temperature, degradation by hydrogen, fracture toughness parameter Jic, CTOD etc. are discussed in literature view in chapter2.A brief experimental study about HSLA80 steel microstructure and its mechanical properties were reported in chapter3. The fatigue precracking of SENB samples required for further fracture study has been presented in chapter4. Experimental study of monotonic fracture toughness test in air and hydrogen environment were reported in chapter5. Comparison of test results in both the environment through Jic and CTOD and Factographic study are presented in chapter6. Main conclusions drawn out with summary and future work were reported in chapter7. References used in the present study are listed in the last chapter.

CHAPTER 2

LITERATURE REVIEW

CHAPTER 2

LITERATURE REVIEW

2.1 Introduction

Hydrogen embrittlement is defined by untimely brittle fracture due to presence/effect of hydrogen. The damage occurred in high strength steel due to hydrogen diffusion in many industry have such a big loss due to hydrogen entrapment in metal is biggest problem in the corrosion field. High strength low alloy steel (HSLA), Cu containing low carbon steels are emerging material for naval and other structural application because of their good combination of high toughness and strength and good weldability. The lower concentration of carbon improves the weldability. The addition of copper provides the required strength through ageing. By different heat treatment process this steel provides various combinations of toughness and strength. Microstructural engineering by thermo-mechanical controlled process (TMCP), along with accelerated controlled cooling (ACC) in this steel can optimize the desired microstructural constituents. The optimization of different microstructural constituents can also be achieved through different processes like rolling and ageing, normalizing and ageing, quenching and ageing. The interaction between hydrogen and steel is the main focus of recent research to analysis hydrogen diffusion in quench and tempered high strength low alloy steel.

2.2 Hydrogen Assisted Cracking

The report of hydrogen effect on mechanical properties in metals was first observed in 1926, by PFEIL [1]. He showed that the presence of hydrogen give remarkable loss in ductility in high strength metal in room temperature beneath static load condition. The chief advantage of HSLA steel is that is proper combination of toughness and strength and also weldability so that the demand of this steel is for construction area with large scale welded structure. The application of high strength low alloy steel is especially in ships, pipeline, naval vessels and offshore facilities. The manufacturing process of high strength low alloy steel is in quench and tempered and direct quench and tempered process as a thermo mechanical controlled process (TMPC). For increasing the strength, precipitations hardening is employed with copper. Hydrogen is much more sensitive toward quench and tempered steel that's why maximum loss occurs in HSLA steel when used in hydrogen environment [4]. Hydrogen embrittlement has been leader of several failure of high strength low alloy steel used in

construction of offshore industry [5]. The problem arises because of hydrogen consumption from sea water which increases when cathodic protection which is applied to the steel to control corrosion. The effect increases when substantiality sulphides are created by active sulphate reducing bacteria in marine construction [6]. Several way to deteriorate the high strength steel by hydrogen is like cleavage, quasi cleavage, ductile fracture micro voids coalescence, brittle intergranular fracture and Trans granular cleavage [7]. There is hydrogen degration from the crack propagation through several ways either internal hydrogen assisted cracking (IHAC) or hydrogen environmental assisted cracking (HEAC). The phenomenon is called Internal Hydrogen Embrittlement and Hydrogen Environment Embrittlement, respectively. Atomic hydrogen is introduced globally while manufacturing operation like welding; casting, heat treatment surface chemical cleaning, and electrochemical machining are done. Chemical reaction and mechanical loading involved in hydrogen environment assists cracking [8].

2.3 History of Ship Building Grade Steel (HSLA Steel)

The development of first high strength steel was in 1960's for naval applications. Ferrite-pearlite steels had been used for many years for high strength structural applications. Medium carbon low alloy steels were also conventionally used for engineering structures in quenched and tempered condition. Advancements in high strength plate steels were stimulated by the demand for (a) high brittle fracture resistance with low impact transition temperature (b) high yield strength (c) greater load bearing capacity with a high degree of weldability [1]. This led to the development of the new series of low carbon steels based on (1) low carbon content (2) good enough alloying elements to that desired transition temperature and (3) microstructural refinement by micro alloying and thermo mechanical processing. In these steels, strengthening mechanisms do not primarily depend on carbon. The strength of this category of steels is due to the dislocation sub-structure and solid solution strengthening [9]. The ultra-low carbon bainitic (ULCB) steel is one category of such steel. A second category is copper containing HSLA steels, which are low-carbon, copper precipitation strengthened low alloy steels. That's why these steels can be provided various combinations of strength and toughness over a broader range of plate thickness. Research on HSLA steels has led to the development of HSLA-80 and the HSLA-100 steel with many publications on the processing, microstructure and properties of these steels [10-11]. For welding problems Copper bearing HSLA steels have been developed. The focus of welding preheat is minimized hydrogen related cracking in the hard martensitic heat affected zone [12]. The relative fabricability of

HSLA-80 in a shipyard production environment has demonstrated significant reduction of fabrication costs [13].

The first certified copper added steel was HSLA80 for naval application by US navy [14]. Later on, with a higher YS, similar toughness and almost equivalent weldability HSLA-100 steel was developed which is a modified version of the copper strengthened HSLA-80 steel.

2.3.1 Physical Metallurgy of HSLA Steel

2.3.1.1 Classification

The different varieties of high strength low alloy steel have been divided in four categories by the American society of metals (ASM) [15];

(a) As hot rolled C-Mn steel with minimum yield strength of 250-400 MPa.

(b) Micro alloyed HSLA steel with properties which result from low alloy additions and controlled hot rolling with minimum yield strength of 275-450 MPa.

(c) High strength structural carbon steels either in normalized or in quenched and tempered condition with minimum yield strength of 550-690 MPa.

(d) Heat-treated structural low alloy steels quenched and tempered with minimum yield strength of 620-690 MPa.

Cu strengthened HSLA steels are the last category of HSLA steels.

2.3.1.2. Roll of Alloying Elements

The HSLA steel properties are controlled by microstructure and micro alloying elements like vanadium (V), titanium (Ti) niobium (Nb) play major role in mechanical properties of these steels. By addition of alloying elements like nickel (Ni), copper (Cu), molybdenum (Mo), chromium (Cr) it improves hardenability, toughness and strength for specific application. The main constituents of copper bearing HSLA steels are combinations of sulphur (S), carbon (C), manganese (Mn), nitrogen (N), silicon (Si), phosphorus (P), Nb, Ti, Cu, Ni, Cr, and Mo in different weight percentages. The carbon level is kept below 0.07 wt. % to control HAZ hardness, toughness and cold cracking, whereas addition of Cu up to 1.5 wt% raises yield and tensile strengths of the steel [16]. Cu transmited solid solution and precipitation strengthening in addition to resistance to corrosion. Cr, Mo and Ni improve toughness of the steel. The hardenability of HSLA steel is improved by addition of Ni, Mo, and Mn and corrosion resistance in marine environment is improved by addition of Cu, Cr and Mo [17-18].

- Carbon is one of the cheapest elements, forms interstitial solid solution of iron, conventionally used for increase the strength of steel. It increases resistance to corrosion, raises impact transition temperature, lowers weldability and hardenability. Toughness and Weldability are deteriorated with higher amounts of carbon [19].

- Manganese is one of the important alloying elements, which is added in different categories of steels in a wide range of wt%, depending upon cooling rate, thickness and strength of the products [20]. Mn acts in steel as austenite stabilizer, carbide former and hot-shortness also prevent due to presence of sulphur.

- Silicon is known as a ferrite strengthener. Silicon increases the tensile strength with a marginal loss in ductility and increases impact transition temperature [21]. The roll of Aluminums in steel as a nitrogen and oxygen scavenger [22]. Micro alloying elements like niobium titanium combines with nitrogen and form nitrides or carbonitrides. They act precipitation hardener and grain refiner and increase the strength of the steel [23].

- Phosphorus and Sulphur have deleterious effects on properties of steel. Sulphur causes hot shortness in steel, i.e., brittleness at high temperatures, whereas phosphorus drastically lowers the ductility and is said to induce cold shortness in steel. The percentage of Sulphur and phosphorus should be less than 0.02 wt% for HSLA steels [24].
- Chromium, molybdenum and nickel, affect the hardenability of steel strongly, besides imparting solid solution strengthening. It is reported that Ni up to 3.5 wt% alone or in combination with Cr was initially used to develop HSLA steels [25]. Cr improves corrosion resistance property and increases the yield strength. [26]. Mo is used for its effect on continuous cooling transformation characteristics [27]. The amount of Mo addition is dependent on the cooling rate and plate thickness [28]. An increase in Cu addition requires a higher amount of Ni addition. Ni prevents grain boundary segregation of Cu and thus reduces the chances of hot shortness [29].Vanadium; Titanium and niobium are added as micro alloying elements in HSLA steel and act as precipitation hardeners and grain refiners. These micro alloying elements increase strength, ductility and toughness of these steels. Ti, Nb and V are strong carbide and nitride forming elements even at very low concentrations [30].
- Copper draws attention as an alloying element because its effects in steel are manifold. Cu can be used as grain refiner, solid solution and precipitation strengthener [31]. Cu increases the strength in Cu-bearing steels through age hardening and it can

increase the toughness as well as corrosion resistance. Therefore, research on Cu precipitation in steel has been essential for understanding as well as development of newer grades of Cu-containing HSLA steels. Precipitation of Cu in iron base systems has been studied by several investigators [32].

2.3.1.3 Thermo Mechanical and Aging Temperature

The heat treatment of Cu containing HSLA steels involves austenitisation or solution treatment followed by quenching and ageing. The processing technology of the steel comprises thermo mechanical controlled processing (TMCP) followed by tempering or ageing [33-34].The TMCP optimizes the grain size of the microstructure through controlled rolling (CR) at high temperature (>900 ^{o}C) followed by accelerated controlled cooling (ACC). The nature and amount of micro alloying elements affect the controlled rolling. Controlled rolling can be divided into three stages [35].

(a) Deformation around 1080 ^{o}C; i.e. in austenite recrystallization region where coarse austenite is refined through repeated recrystallization due to continuous deformation.

(b) Deformation between 950 ^{o}C-870 ^{o}C in austenite non-recrystallization region where format of deformation bands in non-recrystallized austenite provides additional nucleation sites for transformation.

(c) Deformation in the two phase austenite-ferrite region.

The most important stage in TMCP is accelerated cooling (ACC) or direct quenching (DQ). The grain growth is repressed by rapid cooling from finish rolling temperature. Air cooling after accelerated cooling to room temperature provides self-ageing unlike direct quenching. The results of direct quenching in formation of acicular ferrite and martensitic or bainite at room temperature and ageing of the steel is necessary to obtain suitable combination of microstructure and properties. The cooling rate, plate thickness and steel composition together optimize the properties of these steels [36]. Controlled rolling followed by direct quenching or accelerated cooling leads to a uniform fine-grained structure [37]. Fig. 2.1 shows process of Thermomechanical heat treatment.

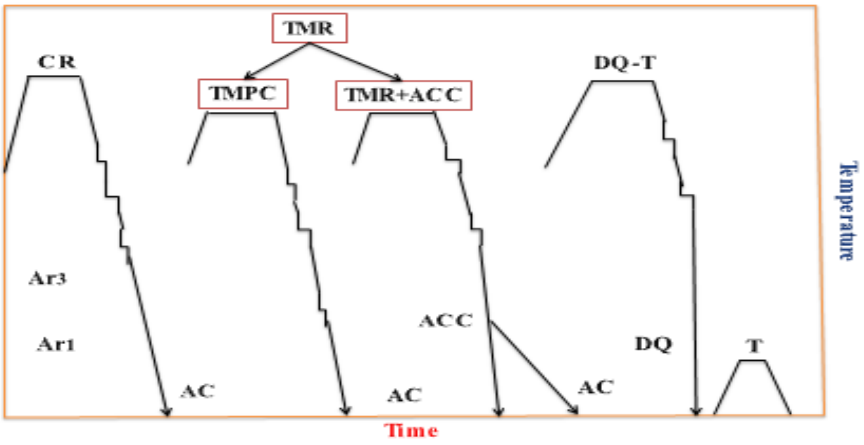

CR: controlled rolling, TMR: thermo mechanical rolling, ACC; accelerated cooling, DQ; direct quenching; T; tempering. AC: air cooling

Fig. 2.1: Schematic representation of different thermo mechanical and heat treatment processing of HSLA steel [33].

2.3.1.4 Strengthening Mechanism

The process variables and alloying elements play an important role in imparting high strength and toughness without impairing weldability and formability of HSLA steels [38].Based on the work of Pickering [39] and Massip et al. [40], the following strengthening mechanisms are thought to contribute in enhancing mechanical properties of HSLA steels.

(a).Grain refinement significantly increases the yield strength and toughness, and lowers impact transition temperature (ITT) of steels. The quantitative relationship between yield strength and grain size has been established by Hall [41] and Petch [42]. Non-recrystallized austenite grains can produce fine grain ferrite where ferrite nucleation rate at the strained austenite grain boundaries are very high but growth rate is low due to space congestion [43]. Starting with a smaller austenite grain size, refinement of ferrite grain size can also be achieved [44].

(b).Solid solution strengthening is dependent on the atomic size differences between solute and solvent. Potent interstitial solutes cannot be used for strengthening to a great extent due to their limited solubility. The influence of the solutes towards strengthening has been studied by Leslie [45]. At small concentrations, the solute has little effect on ductility and the variation in impact transition temperature [46].

(c).Precipitation strengthening is responsible for decrease in impact transition temperature (ITT) [46]. It is also reported that a balance in precipitation strengthening and grain refinement increases the strength and toughness of HSLA steels [47]. The stress required to move dislocations in a slip plane has to be higher than the stress needed to generate dislocations from a source in precipitation strengthened alloys. Therefore, the yield strength associated with the stress required for dislocations to sweep out in the slip planes are large compared with dispersion strengthening.

2.3.1.5 Microstructural Evolutions

The thermo-mechanical processes and alloying elements control the microstructures of Cu-strengthened HSLA steels. It is from this premise that the concept of microstructural engineering arise. The formation of different phases in HSLA steel like acicular ferrite, martensitic, bainitic-ferrite, martensitic-austenite (MA) constituents depend on the mechanism of the transformation kinetics of austenite that in turn is dependent on several factors like transformation time, temperature, amount of deformation etc. Roberts et al. reported the kinetics of austenite transformation from ferrite-pearlite and ferrite-carbide aggregates [48]. The morphology of ferrite is dependent on the transformation temperature, austenite composition and hardenability [49]. Acicular ferrite forms on continuous cooling at a temperature range, which is moderately greater than the bainitic transformation temperature range [50]. Bainite forms between the temperature range of martensite and ferrite-pearlite transformation. It consists of an aggregate of acicular ferrite and carbides. There are various forms of bainite like inverse bainite, granular bainite, lower bainite and upper bainite described in details by Bhadeshia [51].

2.3.1.6. Mechanical Properties

The mechanical properties of HSLA steels are dependent on the chemistry of materials, process parameters, rolling condition, ageing or heat-treated condition etc. that influences the resultant microstructure. The chemical compositions (wt %) of HSLA steel are shown in below table [52];

Table 2.1: Typical HSLA steel chemical composition (in wt. %)

Ni	Si	V	S	Mn	Al	Nb	C	P	B	Ti	N	Fe
0.170	0.25	0.058	0.002	1.70	0.029	0.033	0.08	0.021	0.0024	0.026	0.0048	Rest

2.4 Hydrogen Embrittlement Mechanism

The hydrogen related deterioration are introduced through the processes like (1) hydrogen enhanced dislocation formation leading to dense configuration and high dislocation densities. (2) This dislocation interaction can create vacancies (jog drag and associated with climb effect). (3)The vacancy get decorated and established (reduced the free energy formation).(4) This Nano voids can coalescence and condensate at interferences, interferences junction, twins or cell walls. (5)The void can grow further to from larger voids. The most common hydrogen embrittlement mechanism is the formation of bubbles in high pressure, decreases in surface energy (adsorption mechanism), lowering in the lattice cohesive force (decohensions mechanism) with interaction of hydrogen with dislocations and hydride formation. The embrittlement is manifested by brittle fracture mode, reduced ductility and reduced tensile strength.

2.4.1 Hydrogen Enhanced Decohensions

To explain hydrogen embrittlement a variety of mechanisms have been studied. Indeed within a proposed system depending on the applied stress nature and on the origin of hydrogen the mechanism may also change. The following suggested by Birnbaum [53]: "the forming systems of Non-hydride such as nickel and iron alloys which are not form hydrides conditions under the in which they are fail by loss of ductility because hydrogen reduced the atomic bonding of metals (decohensions)". Hydrogen embrittlement effects are most pronounced in steels. These effects can take the form of embrittlement; ameliorate of crack initiation and propagation, the development of hydrogen-induced damage, such as internal voids and cracks or surface blisters, and in such cases changes in the yield behavior [54]. Hydrogen dissolves moderate extent in all metals. Because of small size of the atom, hydrogen sits in between the metal atoms in crystals of the metal. Followed by it can diffuse also much more rapidly than larger atoms [55]. Dissolve hydrogen (lattice hydrogen) decreases cohesive strength of the lattice.

2.4.2 Adsorption Induced Localized Slip

Crack propagation along with adsorption of hydrogen decreases the surface energy and it results in reduction in fracture stress, weakening of interatomic bonds. Due to this process atom of hydrogen adhere to crack tip and accelerate crack tip dislocation injection by slip processes. This leads to crack growth and introduction of micro voids. This Mechanism was proposed by Lynch. Adsorption of atomic hydrogen at crack tip faces can also lower the surface energy. Hydrogen atoms presumably diffuse into metal near the crack tip and lockup

the mobile dislocation thus preventing the plastic flow. The yield strength increases locally and lack of plastic flow at the tip causes embrittlement [56].

2.4.3 Hydrogen Enhanced Local Plasticity

The regions of high triaxial tensile stress tend to be attracted to where the metal structure is distended. So, it is extended to the regions of notches that are under stress and the ahead of cracks (Fig. 2.2). The hydrogen dissolve in metal that increases the crack, possibly by making cleavage fracture possible by encouraging in the development of intense local plastic deformation. These effects guide to embrittlement of the metal by the cracking which may be Transgranular. The first mechanism was proposed by Birnbaum et al. In some cases hydrogen embrittlement fracture definition is related to losses of microscopic ductility (reduction in area and elongation). But by careful Fractographic examination used by high resolution technique shows hydrogen embrittlement process in steel is concerned with locally enhanced plasticity in the crack tip. In hydrogen under an applied stress distribution can be highly dissimilar, thus, can reduce local the flow of stress, and the result is localized deformation that leads to higher localized failure by ductile processes [57].

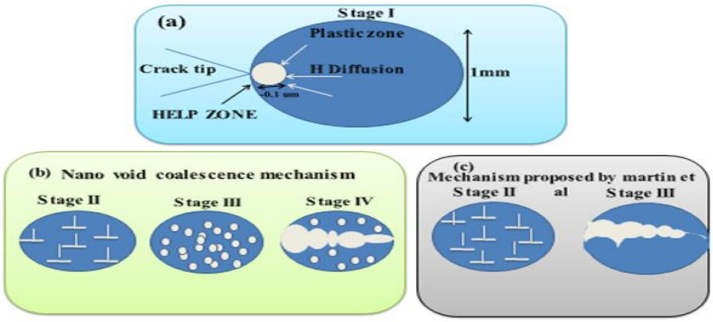

Fig. 2.2: Hydrogen Enhance Localized Plasticity Mechanism Proposed By Martin [63].

(a) stage-HELP zone, excess vacancy accumulation, and vacancy induced growth Nano voids and nucleation.

(b) stage-Hydrogen accumulation weaken HELP zone, decohensions, Nano scale mound, fracture surface mating.

2.5 Fracture Toughness Parameter

Fracture toughness defines test measurement of resistance of a material which leads to crack extension. A test may either a single value of fracture toughness or a resistance curve, where toughness parameter J and CTOD is plotted against crack extension. Cleavage fracture actually has a falling resistance curve. The first standards for J testing were developed in

1970 by ASTM while BSI published the first CTOD test method in 1979 [58]. Some examples of fracture based failures were: a molasses tank explosion of 1919 in Boston, the cracking of Liberty ships during World War II, rocket motor case failures in the space program [59]. Elastic plastic fracture mechanism (EPFM) is domain of fracture analysis which considers extensive plastic deformation ahead of crack tip prior to failure and it is well known as J integral (J) and CTOD.

2.5.1 J –Integral

The J-integral was first proposed by rice (1986). Here, the appearance of growing cracks should be reported. The growth of crack in initial position can be obtained by initial crack and by using of J value plot with the Δa crack growing can be measured. The applicability of J-*I*ntegrals to measurement of crack impelling force while crack extension can be presented in *J* vs. delta *a* sets of values. Usually, *J* values for growing cracks are obtained in laboratory environment following standardized experimental procedures, such as ASTM E1820 [60]. The J integral define as a line integral (path-independent) round through the crack tip. It has widely used in elastic plastic fracture mechanism. J shows the rate of change of net potential energy with respect toward crack advancement (per unit thickness of crack front) for a non-linear elastic solid.

2.5.2 Crack Tip Opening Displacement (CTOD)

The CTOD test standard was first published in Great Britain (1979) [61]. ASTM recently published E 1820, an American version of CTOD standards**.** The crack tip opening displacement that depends on distance from the crack tip. When material failure occurs with such a large deformation, CTOD fracture toughness test performed. This allows the tip of a crack to extended and then open, hence 'tip opening displacement'. The linear elastics fracture mechanics (LEFM) is not valid in CTOD. Crack tip opening is automatically recorded with load verses displacement when test is started.

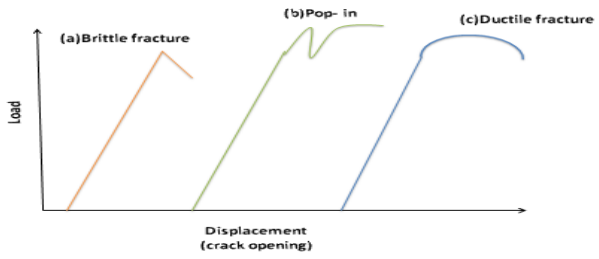

Fig. 2.3: Crack tip opening displacement in different fracture

2.6 Method to Determine J_{IC} (J-R CURVE) and CTOD

A Roman numeral subscript indicates the fracture mode and there are three modes of fracture are illustrated in the images. Mode I fracture is the condition in direction of loading parallel to crack tip opening. This is the most commonly facilitated mode. The direction of loading relative to the crack like defect depends on mode of opening and orientation of loading. There is three mode of crack opening- (1).loading perpendicular to the crack plane called mode first. (2) Loading in plane shear or sliding. (3) Loading along plane of crack and parallel to crack plane. Fracture toughness determined in according to this test to for opening mode I loading.

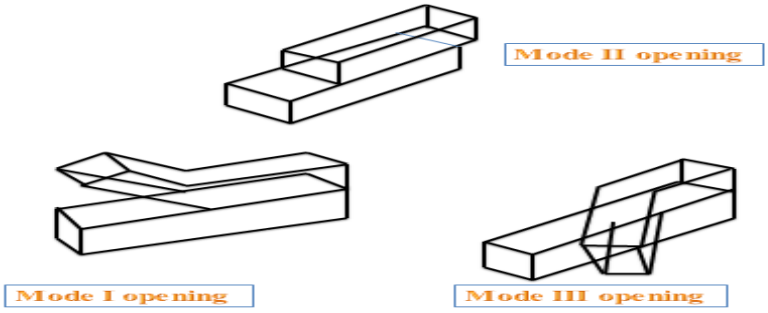

Fig. 2.4: Mode of fracture according to load direction

2.6.1 Resistance Curve Method

Since the fracture properties were estimated by the overall energy consumption, it cannot differentiate different steps of crack initiation and propagation, it is thus necessary to monitor the crack growth behavior (position of the crack tip or crack length) during loading. Practical and well known methods are ‘unloading compliance’ and ‘potential drop’ methods [62]. Unloading lines are used for estimating ‘crack length’ based on the formula given by ASTM E1820-11 [60].

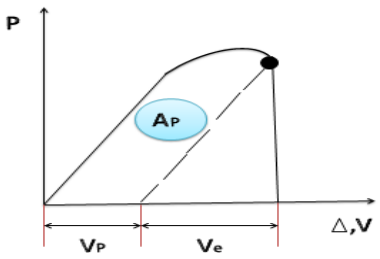

Fig. 2.5: Definition of plastic area under load displacement curve [60].

Step1: calculation of crack size (ai)-

$$u = \frac{1}{\left[\frac{\text{BeWECi}}{S/4}\right]^{1/2} + 1} \quad \ldots. (2.1)$$

$$ai/w = [0.999748 - 3.9504u + 2.982u^2 - 3.21408u^3 + 51.51564u^4 - 113.031u^5] \quad .... (2.2)$$

Step2: calculation of stress intensity factor Ki (mpa-√m)-

$$f\left(\frac{ai}{w}\right) = \frac{3\left(\frac{ai}{w}\right)^{\frac{1}{2}}\left[1.99 - \left(\frac{ai}{w}\right)\left(1 - \frac{ai}{w}\right)\left(2.15 - 3.93\left(\frac{ai}{w}\right) + 2.7\left(\frac{ai}{w}\right)^2\right)\right]}{2\left(1 + 2\frac{ai}{w}\right)\left(1 - \frac{ai}{w}\right)^{\frac{3}{2}}} \quad \ldots. (2.3)$$

$$Ki = \left[\frac{PiS}{\left(BB_N\right)^{0.5} W^{\frac{3}{2}}}\right] f\left(ai/w\right) \quad \ldots. (2.4)$$

Step3: calculation of crack size increment and remaining ligament-

$$a_{(i-1)} = \left(a_i - 1\right), b_{(i-1)} = \left(b_0 - 1\right)$$

step4: calculation of J integral- J elastic part and plastic part

$$J = J_{el} + J_{pl} \quad \ldots. (2.5)$$

$$J_i = \frac{\left(Ki\right)^2\left(1 - v^2\right)}{E} + J_{pl} \quad \ldots. (2.6)$$

Step5: Calculation crack extension (Δa) - The value of J_Q is very dependent on the aoq used to calculate the $\triangle a_i$ quantities by identifying the Ji and ai pair before maximum force reached calculate crack incremental rate.

$$a = a_{oq} + \frac{J}{2\sigma_Y} + BJ^2 + CJ^2, \triangle a_i = \left(a_i - aoq\right) \ldots. (2.7)$$

Step6: Calculate the experimental crack mouth opening displacement compliance from following equation

$$C_i = \frac{6S}{EWB_e}\left(\frac{ai}{w}\right) \times \left[0.76 - 2.28\left(\frac{ai}{w}\right) + 3.87\left(\frac{ai}{w}\right)^2 - 2.04\left(\frac{ai}{w}\right)^3 + \frac{0.66}{\left(1 - \frac{a_i}{w}\right)^2}\right] \quad \ldots. (2.8)$$

Step7:calculate plastic part of load line displacement(V_{pli},$V_{pl(i-1)}$)-

$$v_{pl(i)} = v_{(i)} - \left(P_{(i)}C_{(i)}\right), v_{pl(i-1)} = v_{pl(i)} - 1$$

Step8: calculation of increament of plastic area under the chosen force versus plastic displacement Record between lines of constant plastic displacement at points *i*−1 and *i*.

$$A_{pl(i)} = A_{pl(i-1)} + \left[P_{(i)} + P_{(i-1)}\right]\left[V_{pl(i)} - V_{pl(i-1)}\right] / 2 \quad \text{…. (2.9)}$$

Step9: calculation of j- plastic by this formula

$$J_{pl(i)} = \left[J_{pl(i-1)} + \left(\frac{\eta_{pl(i-1)}}{b_{(i-1)}}\right)\left(\frac{A_{pl(i)} - A_{pl(i-1)}}{B_N}\right)\right] \times \left[1 - \gamma_{pl(i-1)}\left(\frac{a_{(i)} - a_{(i-1)}}{b_{(i-1)}}\right)\right] \quad \text{…. (2.10)}$$

Plastic constant factor n (i-1) = 1.9, y=0.9(i-1), Add both part of J integral

$$\eta_{pl} = 3.667 - 2.199\left(\frac{a_{(i-1)}}{w}\right) + 0.437\left(\frac{a_{(i-1)}}{w}\right)^2, \gamma_{pl} = 0.131 + 2.131\left(\frac{a_{(i-1)}}{w}\right) - 1.465\left(\frac{a_{(i-1)}}{w}\right)^2 \ldots.$$

(2.11)

Step10: Finally using the J value for CTOD calculation in expression –

$$\delta_i = \frac{J_i}{m\sigma_y}, \; m = A_0 - A_1 * \left(\frac{\sigma_{YS}}{\sigma_{TS}}\right) + A_2 * \left(\frac{\sigma_{YS}}{\sigma_{TS}}\right)^2 - A_3 * \left(\frac{\sigma_{YS}}{\sigma_{TS}}\right)^3 \quad \textbf{…..}(2.12)$$

$$A_0 = 3.18 - 0.22 * \left(\frac{a_i}{w}\right), A_1 = 4.32 - 2.23 * \left(\frac{a_i}{w}\right), A_2 = 4.44 - 2.29 * \left(\frac{a_i}{w}\right), A_3 = 2.05 - 1.06 * \left(\frac{ai}{w}\right)$$

Constructing the J-R Curve:

The J-Rcurve is defined as the data in a region bounded by the Jmax and Δa max.

- First graph is plotted between J vs. da by calculated value. The initial point of curve is picked up where plastic crack extension start. Then it is cut before the chosen initial point and again plot curve.
- The construction line is determined by the following equation-

  $$J = 2\sigma_Y \triangle a \quad \text{…. (2.13)}$$

- The construction line is plotted and 0.15 mm exclusion line parallel to construction line is drawn. Then 0.2 mm offset lines parallel to construction line is drawn.
- Finally 1.5 mm exclusion line parallel to construction line is plotted.
- The line intersects of 0.15 mm exclusion line vertically down point is called min. crack extension and line where 1.5 mm exclusion line intersect is taken as crack extension limit.
- 0.2 mm offset lines intersect point called J_Q point.

- After checking of the validity criteria J_Q become equivalent of J_{IC}.
- Same procedures are followed for plotting the CTOD. Construction line expression for CTOD are;

$$\delta_i = 1.4 * \Delta a \quad \text{…. (2.14)}$$

Important Criteria for J-R Curve (J_Q Qualification)-

(a)Before Stable Tearing Fracture Instability –before stable tearing crack extension fracture occurs $\Delta a_p < 0.2mm + J_Q / 2\sigma_Y$

(b) After Stable Tearing Fracture Instability –after stable tearing crack extension fracture occurs $\Delta a_p > 0.2mm + J_Q / 2\sigma_Y$

J maximum-

$$J_{\max} = b_0\sigma_y / 10$$

The maximum crack extension capacity -

$$\Delta a_{\max.} = 0.25b_0$$

Limit-

$$J_{\text{limit}} = b_0\sigma_y / 7.5$$

FOR CTOD (δ-R) CURVE

Calculation of δi requires- $\sigma_{YS} / \sigma_{TS} > 0.5$

The maximum δ capacity -

$$\delta \max. = b_0 / 10m$$

The maximum crack extension -

$$\Delta a_{\max.} = 0.25b_0$$

Limit-

$$\delta_{\text{limit}} = b_0 / 7.5m$$

Relation between CTOD and J-

$J = m\sigma_y\delta$ Where m is constant value between 1to 2, σ_y flow stress.

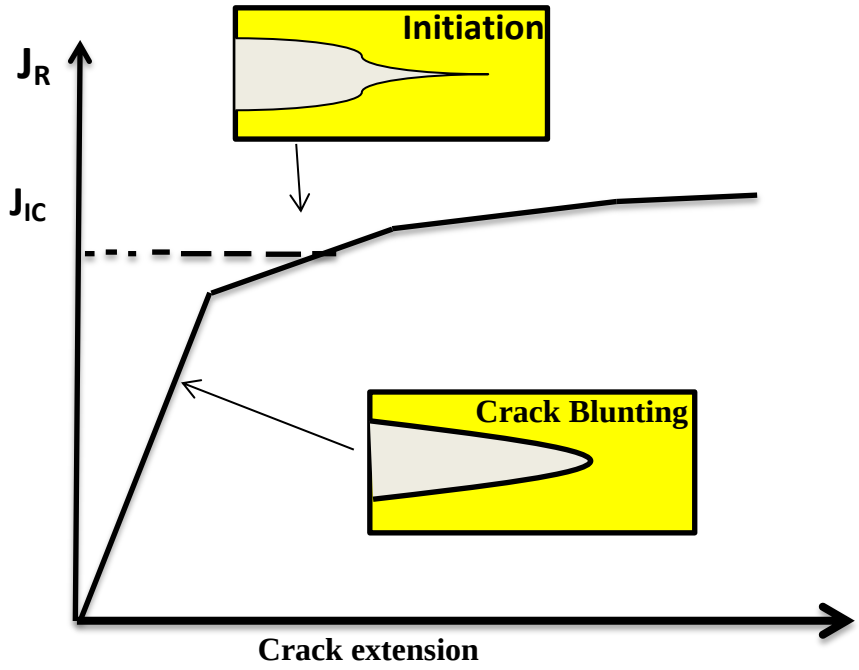

Fig. 2.6: Typical J-R curve for ductile material

Fig. 2.6 shows how the crack opening and crack blunting line indicates that before failure, elastic deformation occurs then plastic deformation start and it means crack initiation start value is the fracture toughness value of material. It also informs about the energy absorb capacity of material before its fracture. Crack blunting line is constructed through different available methods. Linear elastic plastic failure mechanism studies are used for upper self. By studying this Fig. one can also conclude about the fracture type (ductile or brittle) and before failure how much deformation has occurred.

CHAPTER 3
CHARACTERIZATION OF HSLA-80 STEEL

CHAPTER 3

CHARACTERIZATION OF HSLA-80 STEEL

3.1 Introduction

HSLA80 steel was certified for uses of ship construction and defense departments are implementing this type of steel for their ship building. Apart from high strength and lower weight, the remarkable factor of HSLA-80 steel is its weldability.HSLA80 steel is a primary structural steel used in construction of the new Arleigh Burke Class destroyers, Ticonderoga class cruisers, in some structure of the later Wasp Class amphibious assault ships and Nimitz Class aircraft carriers.HSLA80 steel is a low carbon, copper precipitated strengthened steel based on ASTM A710steel.

3.2 Experimental procedure

3.2.1 Material composition

H.S.L.A.80 (High Strength Low Alloy Grade-80) steel used in the present study had nominal composition as below. Heat treatment history of the as recived material consisted of spray quenching 600^0C followed by tempering in 800^0C.

Table3.1: Composition of HSLA80 steel (wt. %)

C	Mn	Nb	Al	V	Mo	Si	Ni	Cr	Cu	S	P	Fe
0.05	1.00	0.037	0.025	0.06	0.51	0.34	1.77	0.61	1.23	0.001	0.009	Rest

3.2.2 Material characterization

X-ray diffraction (XRD) studies of high strength low alloy 80 steel were performed by Philips X-pert system. X-ray diffraction were carried out with scan rate of 3^0/minute in 2θ range of 10^0-$100^0$with Cu target.

Fig. 3.1: Philips XRD system

For microstructural observation the steel sample was prepared by standard micrographic sample preparation process. Optical and Scanning electron microscope (SEM) was utilized to study the microstructure of HSLA80 steel. The sample used for the observation is taken from SENB sample. HSLA80 specimen was subjected to Vickers hardness testing with 5kgf load. The indentations were taken three times in each specimen and average hardness values have been reported. The tensile properties of HSLA-80 steel were obtained by tensile test conducted as per ASTM standard using 100KN Instron servo electric testing machine in two different cylindrical specimens. A constant displacement rate of $3\mathbf{x}10^{-3}$ mm/s, with a gauge length 25mm was employed with extensometer attachment. SEM photograph of the fracture surface was captured to study the fracture mode.

3.3 Results and discussion

(a) XRD analysis

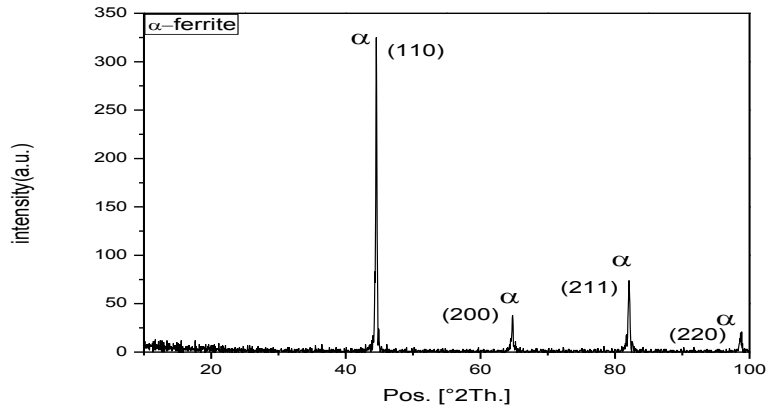

Fig. 3.2: XRD result of HSLA80 steel.

Fig. 3.2 shows XRD plot of the as received steel and it only represents BCC peaks as expected. This may be due to presence of ferrite or martensite. Any appreciable FCC peak of retained austenite could not be ascertained.

(b) Microstructural observation

Fig. 3.3 shows the optical micrograph of the as recived steel at different magnification. As the received steel was in found quenched and tempered condition, the Fig. shows tempered martensite,acicular ferrite,bainite and retained austanite. found.that is same condition with quench and tenpered steel.the investigated of material were as the receive condition.

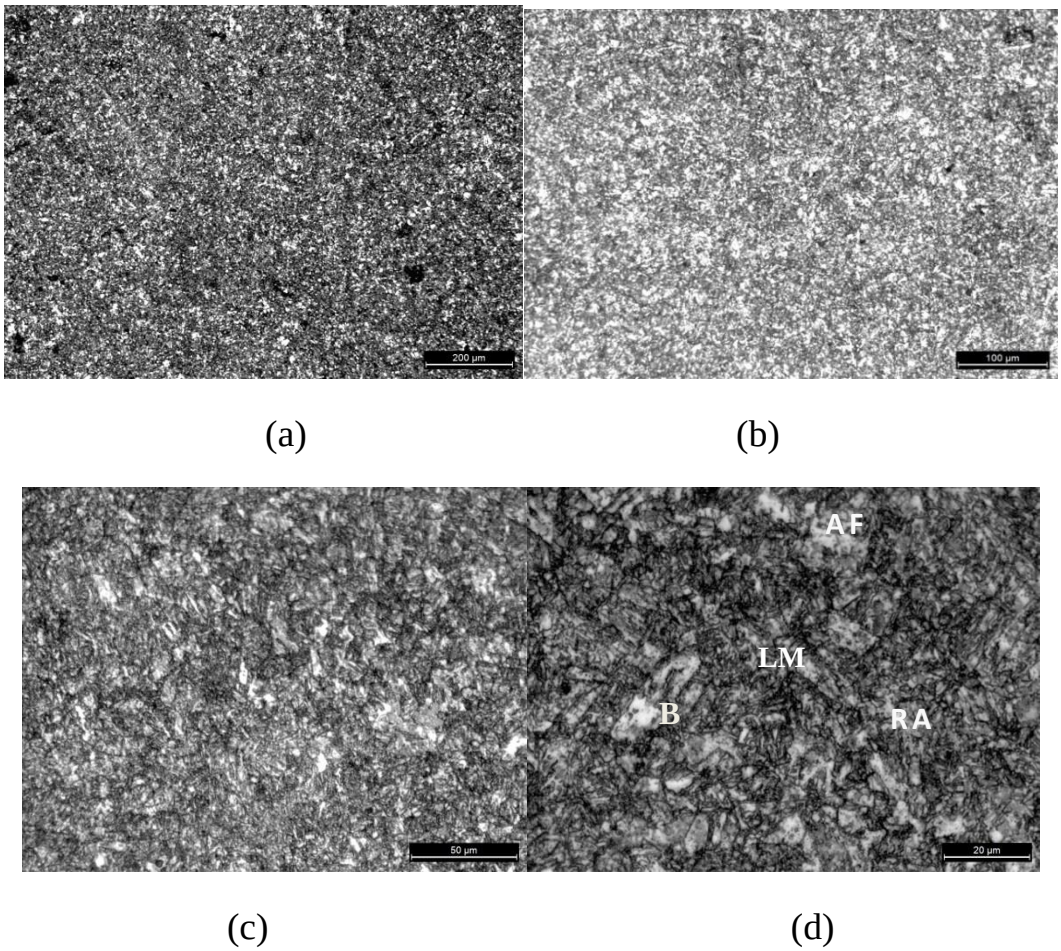

Fig. 3.3: Optical micrograph of HSLA 80 Steel at (a)10x, (b)20x, (c)50x and (d)100x magnification.

Note: AF acicular ferrite,LM lathe martensite,B bainite,RA retained autenite.

(c) Mechanical properties

Hardness

Hardness test result of the as recived steel is tabulated in the table 3.2

Table3.2: Hardness test result of HSLA80 specimen

Vickers Hardness (5kgf)			Average
Reading 1	Reading 2	Reading 3	
219HV5	222HV5	219HV5	220HV5

Tensile properties

Engineering stress strain plots of the tensile testing are displayed in Fig. 3.4 and the results are displayed in tabular form in table 3.3.From the Fig. and the table it can be observed that the steel has good elongation properties.

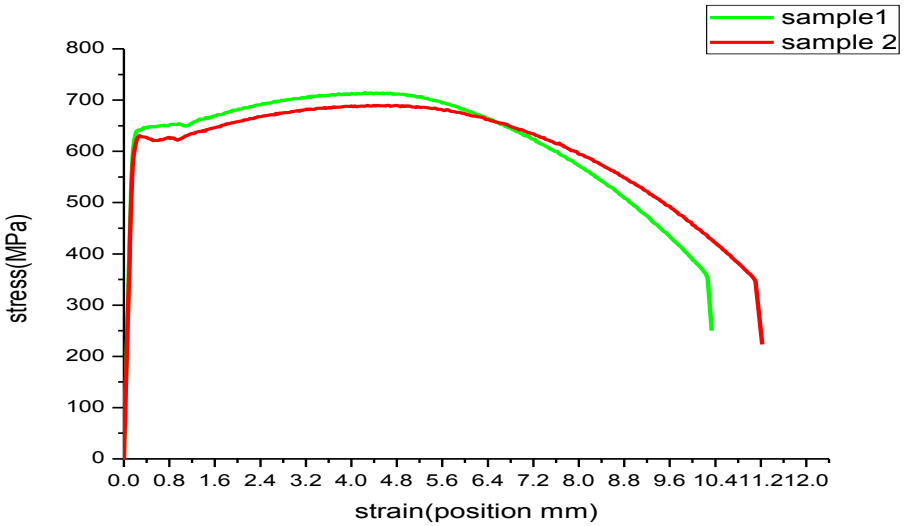

Fig. 3.4: Engineering stress strain plot of HSLA-80 specimens

Table3.3: Tensile properties of HSLA80 steel

Sample	Yield strength(MPa)	Tensile strength(MPa)	Elongation (%)	Reduction in area (%)	Poisson ratio	YS/UTS
Sample 1	648.78	714.64	23.66	76	0.3	1.03
Sample 2	627.27	689.94	20.9	81.9	0.4	0.90

Fractographic study

After tensile testing fracture surface was studied by SEM. Related micrographs are shown in Fig. 3.5. Fig 3.5(a) shows cup and cone fracture appearance due to good ductility of the steel. From Fig. 3.5 (b & c), where higher magnification fractograph were shown it is clear that the fracture surface mainly consists of dimples. It can be concluded that the fracture modes were due to micro void coalescence and ductile in nature fracture.

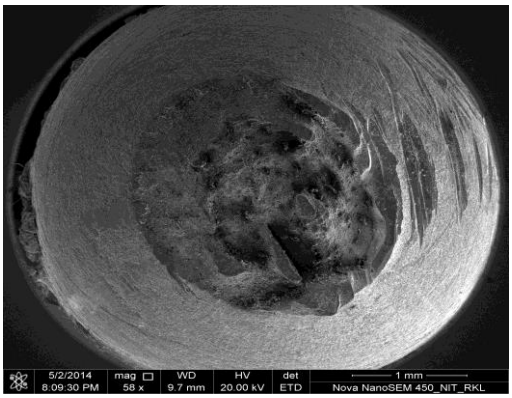

(a)

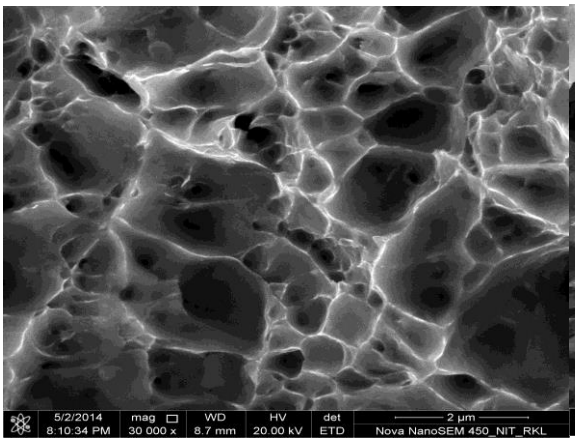

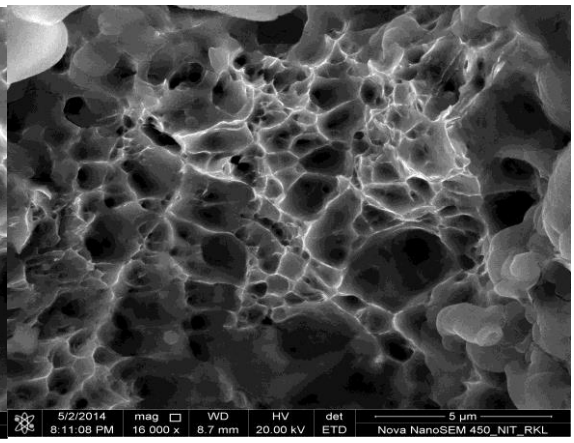

(b) (c)

Fig. 3.5: (a) Cup and cone fracture of HSLA80 specimen

(b) and (c) higher magnification fractograph of HSLA80 specimens

3.4 Conclusion

By the tensile test of the specimen it was observed that the yield strength and ultimate tensile strength of HSLA80 steel is better than other common alloy steel. SEM image shows the ductile failure of specimen due to presence of cup and cone morphology and dimples. It was also observed that large plastic deformation occurs before failure. Thus HSLA80 steel is ideally used for structural application.

CHAPTER 4

FATIGUE PRECRACK OF SENB SAMPLE

CHAPTER 4

FATIGUE PRECRACK OF SENB SAMPLE

Fig4.1: Fatigue precracking of SENB sample in servo hydraulic machine

4.1 Introduction

For fracture toughness testing sharpest possible notch is introduced in the sample and the possible sharpest crack can be generated by fatigue precracking only. So, fatigue precrack is generated on some notched samples like Single edge notch bend (SENB) sample. The test method involves fatigue precrack of already machine notched specimen by loading in three point bent test.

4.2 Experimental procedure

4.2.1. Specimen preparation

For the specimen preparation sample was cut from the steel plate in such a way blanks length is parallel to the direction of rolling to the plate. Single edge notch bend specimens of 150mm (L) x30mm (w) x15mm (B) nominal dimensions were machined notched in L-T orientation. The specimens were designed with the knife-edges at the notch mouth. This notch mouth design was as so that a C.O.D.gauge can be fixed and by the unloading compliance method crack increments can be calculated. Proper measurement of SENB specimen parameter gives less chance of error in experiment. The photograph and schematic geometry of the SENB sample are shown in Fig. 4.2 and 4.3. Here, Initial crack length (ao), Thickness(B), Width

(w), Notch length, Span/roller center distance(s) =4*w and a/w ratio (should be 0.5. of total crack length (a)) are very crucial.

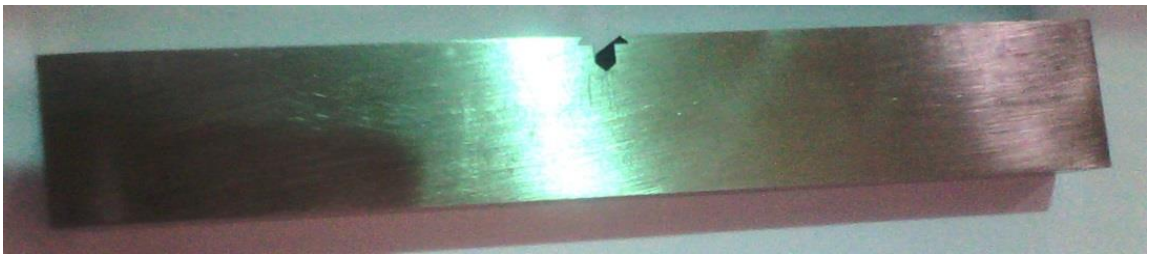

Fig. 4.2: SENB sample

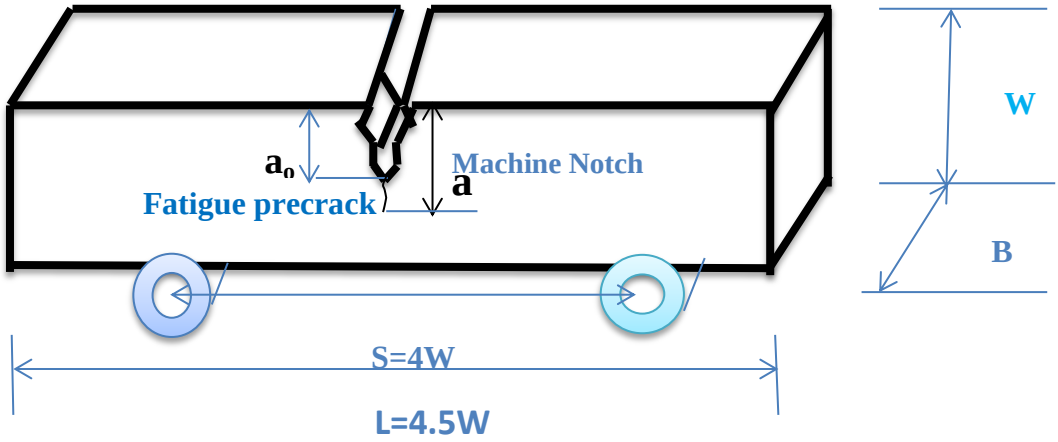

Fig. 4.3: Geometry of SENB specimen with dimensions

4.2.2 Precrack generation

Precrack on S.E.N.B. sample was generated by using servo hydraulic material test system, Model (no.8501, maker-instron, SL.NO.H0488) and C.O.D Gauge/clip gauge (crack opening displacement gauge -Model NO.2670-114, SL.NO.342) with gauge length-5mm, travel 2mm. Fatigue precrack were grown in the specimen in a/w ratio 0.5(where a and the w are crack length and width respectively) by using software control.

In crack tip local stresses are described by stress intensity factor. Before any test started load and strain calibration is necessary. Minimum load was set after making the file for saving the data. Test was started with delta k range in 5 MPa√m to slowly one or two step till maximum 20 MPa√m and then the frequency was changed from 5 to 20 Hz. During this, the mean and amplitude error was checked. The cyclic load used here was compressive in nature. The

specimen was monitored carefully until crack initiation observed. The stress ratio can be observed at a value of 0.1. Stress intensity factor is used predict state of stress near crack tip in fracture mechanism. The applied stress intensity factor is shown in Fig. 4.4.

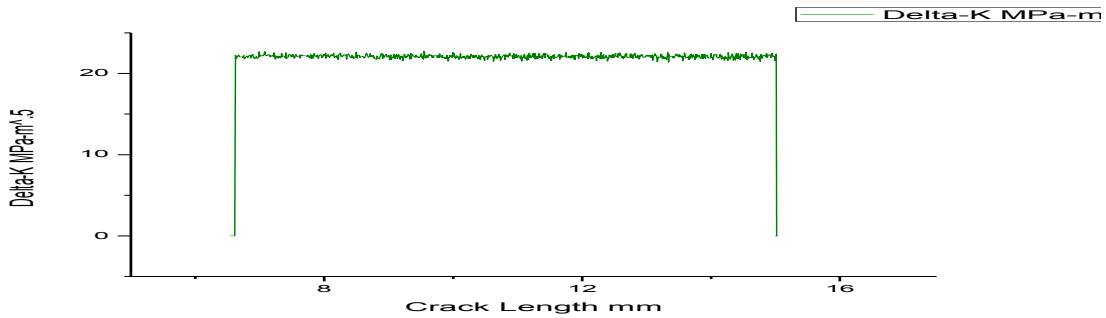

Fig. 4.4: Stress intensity factor range verses crack length during cyclic loading of Fatigue precrack test of HSLA80specimen.

COD gauge used for measurement of the crack opening displacement. The COD are designed to perform as per ASTM and ISO standard fracture mechanics test in both cyclic and static nature and cover all specimen geometry. COD gauge gives precise hints of relative displacement of two accurately located knife edge (machine references edge) which spans the starter notch of specimen. The COD gauge used in the test had 5mm gauge length and travel of 2mm having maximum load and stress intensity control during precracking. The fatigue precrack mainly start with load that give maximum stress intensity factor. This increased after every 10 minute till amplitude and mean error become stable. This step was repeated until the crack grows.

4.3Results and discussion

As first step of the present study, fatigue precracking was done. The fatigue crack growth rates are expressed by function of stress intensity factor range at crack tip. da/dn verses delta k that shows stable crack extension in cyclic loading under change of materials resistance. Details of all samples precracked till a/w ratio 0.5 are shown in table 4.1. Figure 4.5 also shows crack length verses cycle curve of during one precracking.

Table4.1: Result of fatigue precrack of SENB sample with nominal dimensions

HSAL80Single Edge Notch Bend Specimen									
Sample	$\triangle k$ (MPa√m)	Frequency (Hz)	R-ratio	Initial crack (mm)	Final crack (mm)	Span length (mm)	Width (mm)	Thickness (mm)	Notch length (mm)
Sample1	20	20	0.1	6.34	15.013	120.08	30.026	15.12	5.05
Sample2	20	20	0.1	6.778	15.029	120.232	30.058	15.074	5.01
Sample3	20	20	0.1	6.74	15.048	120.384	30.096	15.008	5.13

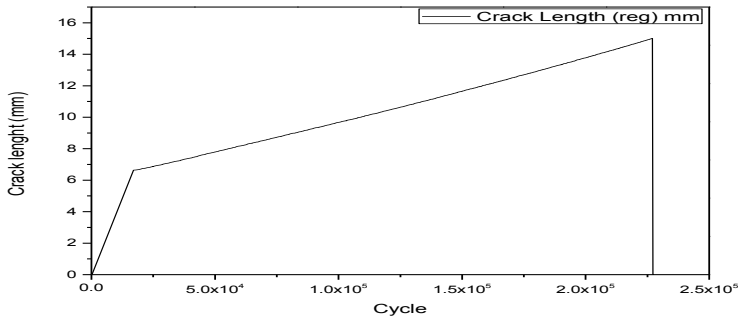

Fig. 4.5: **C**rack length verses cycle curve of precrack SENB sample

4.4 Conclusion

Fatigue precrack is primary requirement of fracture toughness test and in this was carried out successfully. Stress intensity factor range and crack growth rate shows the materials resistance to the stable crack extension under the cyclic loading. Fatigue precrack much beneficial for study the crack growth rate in particular direction and for fracture toughness test.

CHAPTER 5

Monotonic fracture toughness test in air and hydrogen Environment

CHAPTER 5

Monotonic fracture toughness test in air and hydrogen Environment

5.1 Introduction

In this chapter previously precracked SENB specimens were utilized to measure the fracture toughness of the HSLA 80 grade steel by J_{IC} and CTOD approach. Moreover, to study effect of hydrogen the tests were carried out both in air and hydrogen (prepared aqueous solution). The study was carried out at different displacement rates at monotonically increasing load.

5.2 Experimental procedure

5.2.1. Specimen and environment

In this chapter fracture toughness tests were carried with the precracked SENB specimen obtained earlier (described in earlier chapter). Tests were carried out both in air (normal condition) and hydrogen atmosphere. For hydrogen atmosphere the sea water environment was created by NaOH as we intend to study the steel for naval application and by electrolysis of the solution nascent hydrogen was obtained. The solution was prepared by adding 4 g of NaOH in 1 l of distilled water (making the volume) to get 0.1N solution of NaOH. *PH* value was measured by litmus paper and the value measured was 13.20.

In SENB sample one small hole was created for proper holding of a wire connected to DC power supply so that the sample worked like cathode. Platinum electrode was used as anode. During the test 20 V potential was applied. Precharging of hydrogen, i.e. before start of the fracture test hydrogen evolution was started 24 hours before the start of test at room temperature. During the test also the same current and voltage level was continued. Only the precrack portion was in contact with the solution, other part was covered by the Teflon to make that area nonconductive. During the power on condition the negatively charged area, i.e. the precrack portion comes in contact with the evolved hydrogen and that acts as the environment and the same diffuses into the steel. Before start of the test using a marker a line was marked at 1.5 mm above crack tip. While the test solution level goes down, fresh solution was filled to maintain the depth. The schematic diagram of the arrangement is shown in Fig. 5.1.the monotonic J –integral test were carried out in servo-electric test frame with ±30 KN load cell. The specimens were precharge with hydrogen at load corresponding latest value during precracking.

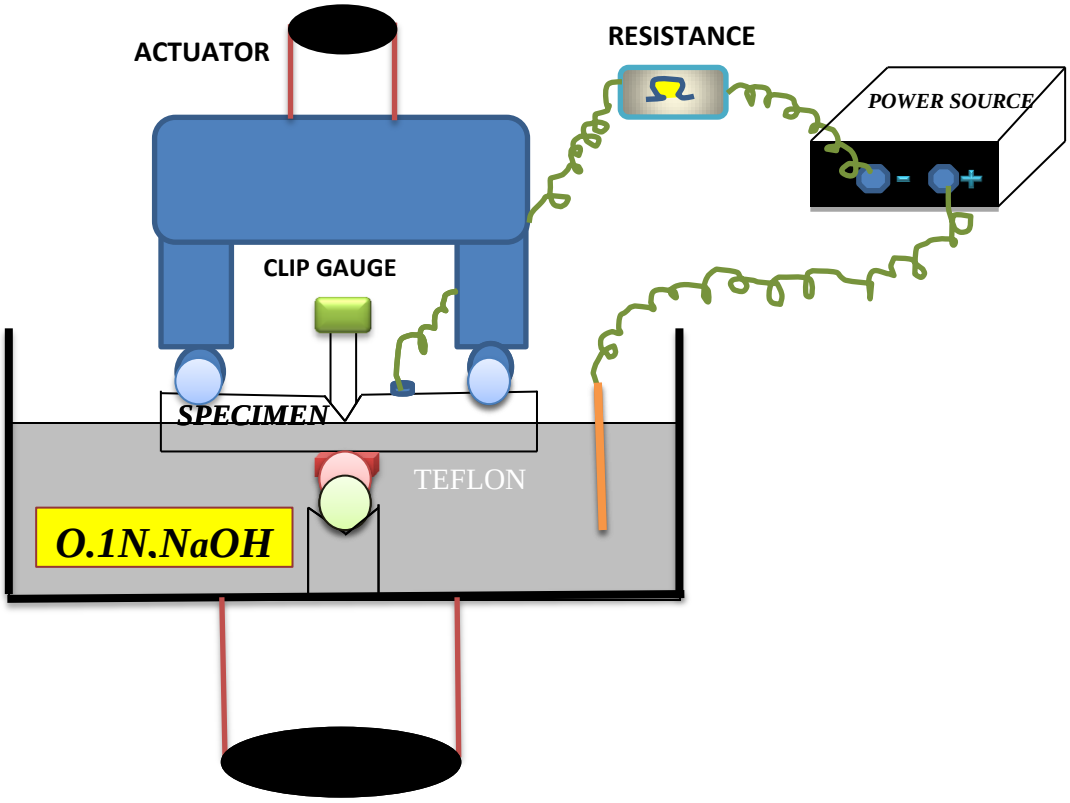

Fig. 5.1: Schematic representation of testing arrangement with hydrogen

5.2.2 Test parameters

Before start of testing load and strain calibration was done. The chosen of displacement rate for fracture toughness test is important criteria. As failure of high strength low alloy steel takes place in very slow displacement rate, it takes long time; so slow displacement rate were chosen to observe the behaviour of material in normal condition and hydrogen environment. First samples were tested in air in room temperatures and the test was conducted in very slow displacement rate of 0.0001mm/s in compressive load condition. The schematic arrangement of cycle generated by monotonic-J software is shown in Fig. 5.2 and 5.3.Loops was used for both the tests and loop divided in three steps:

I. First 0.3mm(-ve)
II. Second0.15mm(+ve)
III. Third0.15mm (-ve)

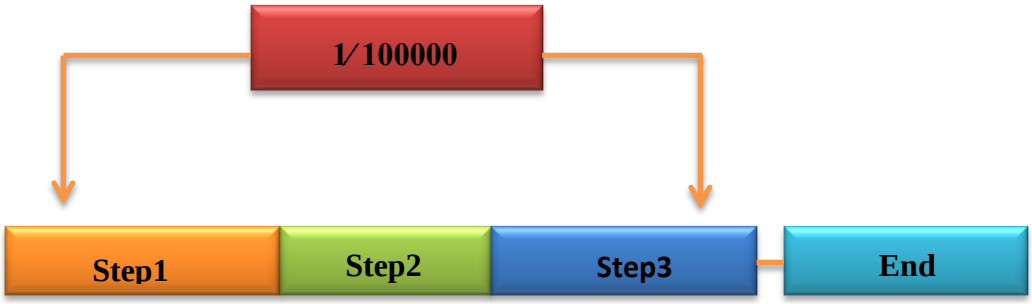

Fig. 5.2: Progressive indicator loop for mono-J test

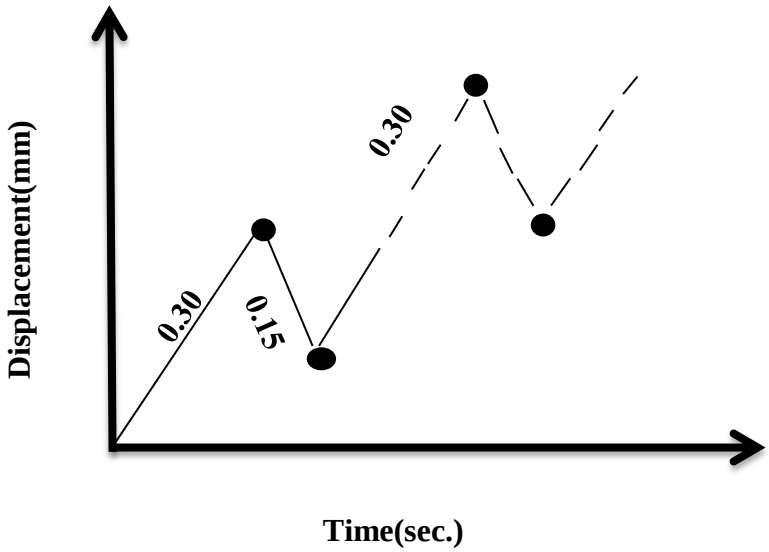

Fig. 5.3: schematic diagram of waveform.

The test specimens were loaded with a waveform as shown in above figure.

5.2.3Monotonic-J test in air

Fig. 5.4: Fracture toughness test in air in servo electric machine with 10^{-4}mm/s displacement rate.

This test was conducted in servo electric machine (Instron, model no.8861).Test was started with same arrangement in instron dynamic software wave maker. Here it was done is displacement control mode and displacement rate was 0.0001mm/s.After the test data was used to calculate the energy required for opening the crack and propagate by using J-integral analysis and formula. The maximum load was -26.2003KN and after that unloading started. Fig: 5.4 shows the load verses position curve and it can be observed that load increases slowly with the displacement rate. When load reached maximum point the crack was opened and then loads starts decreasing as the crack growth rate increases until return to initial position.

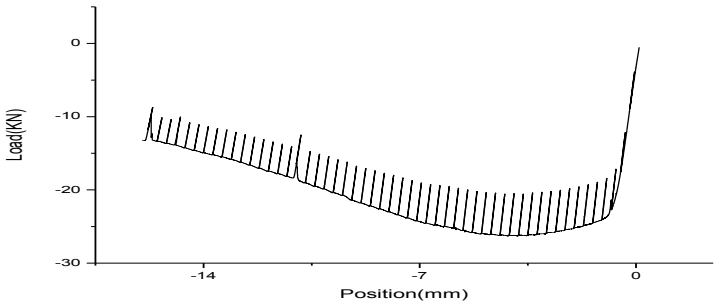

Fig. 5.5: Load-displacement for HSLA80 air at 0.0001mm/s.

5.2.4Monotonic- J test in hydrogen environment

Fig. 5.6: Fracture toughness test in hydrogen environment in servo electric machine

Test in hydrogen environment was carried out with same testing machine as used in air but the sample was immersed in solution as described earlier. Here C.O.D.gauge was used

(model no.2670-114, S.NO.-342, gauge length-5mm, travel-±2.0mm). The compressive load started from -3.0KN and slowly increased and maximum load was -24.322 KN then peak load drops started. Fig. 5.6 shows the load verses crack mouth opening displacement with respect to actuator movement. Fig. 5.7 shows load vs extension plot during the test. Monotically load was applied and displacement was increasing with cycle. It clearly shows that after maximum is load reached (failure crack propagated) unloading was started.

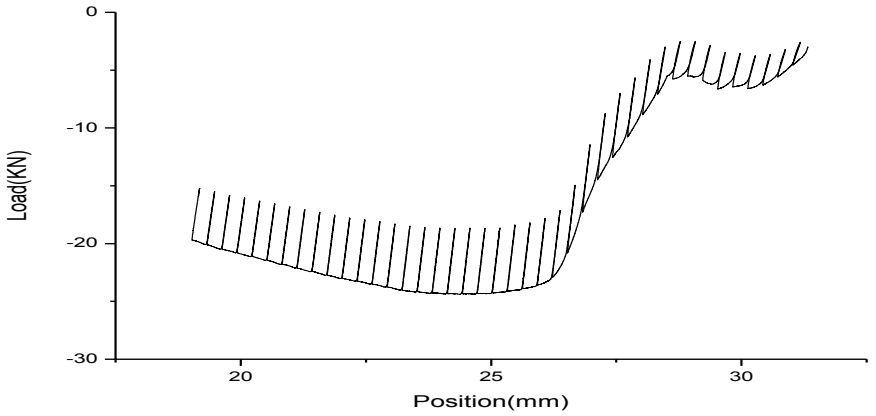

Fig. 5.7: Load- displacement curve of HSLA80 sample tested in hydrogen environment

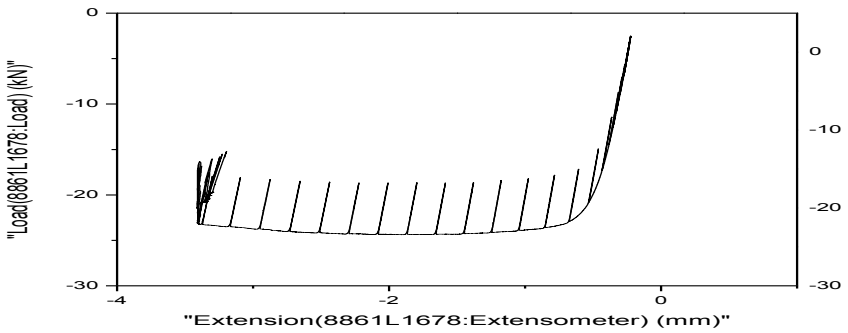

Fig. 5.8: Load vs. COD curve hydrogen environment test in 0.0001mm/s displacement rate

5.3 Results and discussion

5.3.1 Jic and CTOD Result of Specimen Tested In Air

Fig. 5.9: View of fracture SENB sample after mono-J test in air

Fig. 5.9 shows the SENB sample after mono-J test in air. After completion of test data were calculated and analyzed following ASTM E1820-11 standards. Here, the unloading compliance method was used (Fig. 5.9) and the compliance wad calculated by displacement divided by load. All validity criteria were also followed.

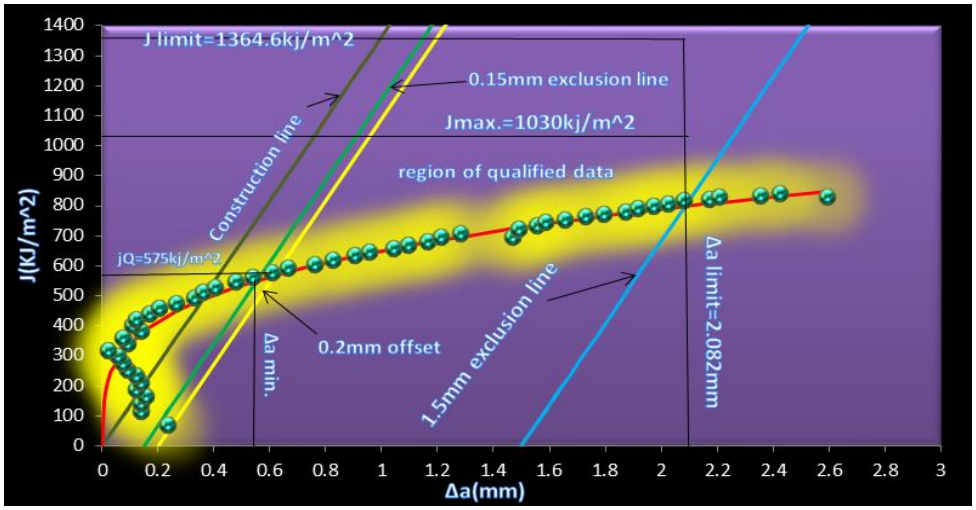

Fig. 5.10: Unloading compliance J-R curve for HSLA80 sample tested in air displacement rate 0.0001mm/s

In Fig. 5.10 the point intersects with 0.2 mm offset line called J_Q point. The validity criteria checked as below:

Data qualification:-

- J_{imit}=1364.6kj/m^2, J_{max}=1030kj/m^2,
- J_Q qualify J_{IC}-(a).thickness $B > \frac{10J_Q}{\sigma_Y}$ = (15.12>8.436)

(b). Initial ligament $b_o > \frac{10J_Q}{\sigma_Y}$ = (15.013>8.436)

(c). $\triangle a_p < 0.2mm + J_Q / 2\sigma_Y$ =2.59<4.21

Condition for fracture instability before the stable tearing –condition for fracture stability before stable tearing crack extension $\triangle a_p < 0.2mm + J_Q / 2\sigma_Y$ =2.082<0.621(not valid)

Condition for fracture instability after the stable tearing –condition for fracture stability after stable tearing crack extension

$\triangle a_p > 0.2mm + J_Q / 2\sigma_Y$ =2.082>0.621(valid)

So that fracture occure after stable tearing

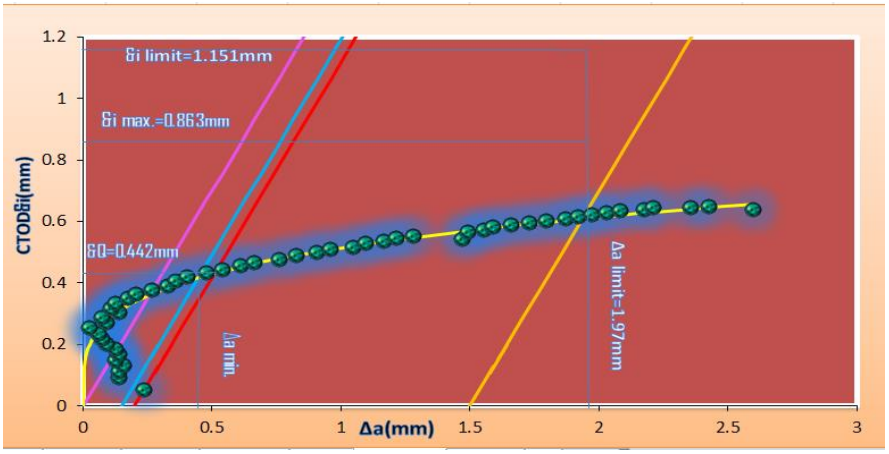

Fig. 5.11: Unloading compliance δ -R curve for HSLA80 sample tested in air

Fig. 5.11 shows the graph of CTOD verses crack extension and it was observed that the crack tip opening was ductile type so fracture occurred in ductile fracture mode.

Data qualification

- $\delta_{\max.} = \frac{b_0}{10m}$ =0.863mm, $\delta_{Q.} qualify \delta_{IC} - b_o > 10m\delta_Q$ = (15.013>5.0905)

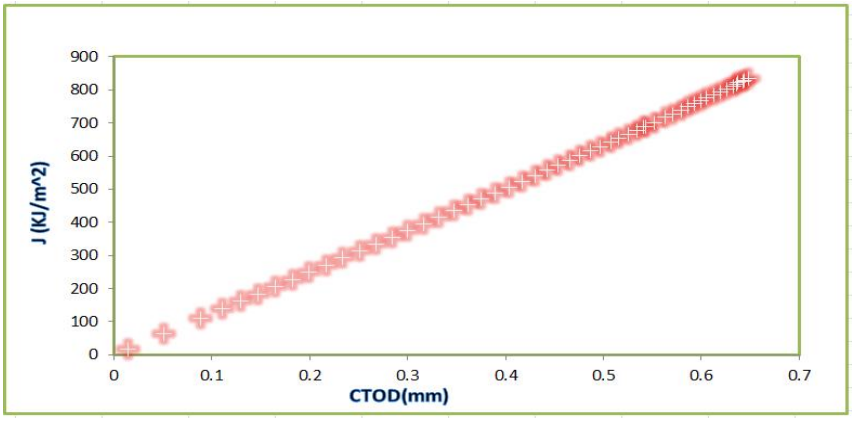

Fig. 5.12: J-CTOD curve for SENB sample tested in air

5.3.2 Jic and CTOD Result of Specimen Tested In Hydrogen Environment

Similar to air, calculation was made for hydrogen environment sample also. Fig. 5.12 shows the unloading compliance curve of the same.

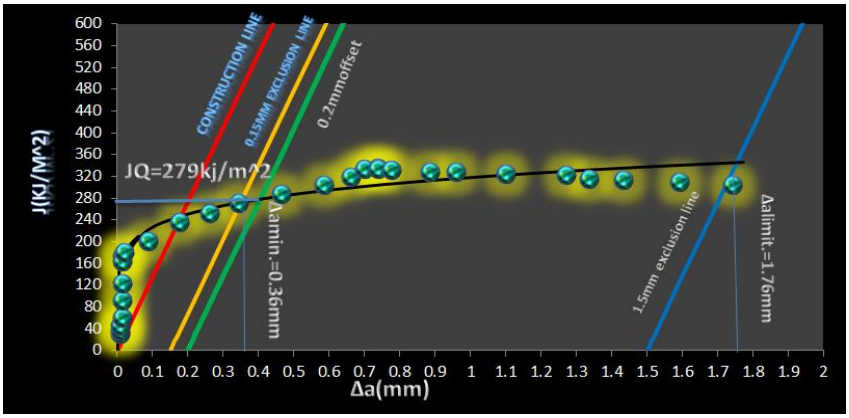

Fig. 5.13: Unloading compliance J-R curve for HSLA80 sample tested in hydrogen displacement rate 0.0001mm/s

- J_{imit}=1366kj/m^2, J_{max}=1027kJ/m^2,
- J_Q qualify J_{IC}-(a).thickness $B > \frac{10J_Q}{\sigma_Y}$ = (15.074>4.0926)

(b). Initial ligament $b_o > \frac{10J_Q}{\sigma_Y}$ = (15.029>4.0926)

(c). $\triangle a_p < 0.2mm + J_Q / 2\sigma_Y$ =1.77<2.04

- **Condition for fracture instability before the stable tearing** -condition for fracture instability before the stable tearing crack extension

  $\triangle a_p < 0.2mm + J_Q / 2\sigma_Y$ =1.76<0.404(not valid)

- **Condition for fracture instability after the stable tearing** -Condition for fracture instability after the stable tearing crack extension

  $\triangle a_p > 0.2mm + J_Q / 2\sigma_Y$ =1.76>0.404(valid)

Above valadity criteria has been checked and obtined fracture occure after stable tearing .

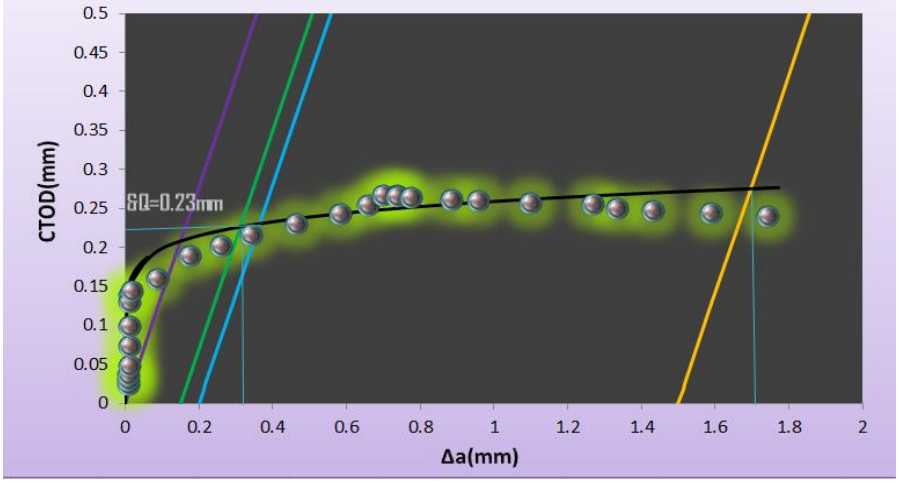

Fig. 5.14: Unloading compliance δ -R curve for HSAL80 sample tested in hydrogen environment

The above graph (Fig. 5.14) showing the crack tip opening is less ductile and so the failure occurs in ductile brittle transition region by the effect of hydrogen.

Data qualification

- $\delta_{\max.} = \frac{b_0}{10m} = 0.9887\text{mm}, \delta_{Q.} qualify \delta_{IC} - b_o > 10m\delta_Q = (15.029 > 6.0101), \delta_{\text{limit}} = 1.152mm$

The performance of J_IC test was calculated with single specimen unloading compliance technique followed by ASTM standards. For HSLA80 specimen the value of J_IC was estimated 575KJm^{-2} in hydrogen environment and in air 279KJm^{-2}**.**

5.3.3 Fractographic study

The fractured specimens were subjected to micrographic and Fractographic study to analyses the type of fracture. Fig. 5.14 shows the photograph of J_{IC} test specimen failed after testing in air. Both for air and hydrogen environment tested samples the crack extension area was studied under SEM. Fractographic images of this area are displayed in Fig. 5.15.

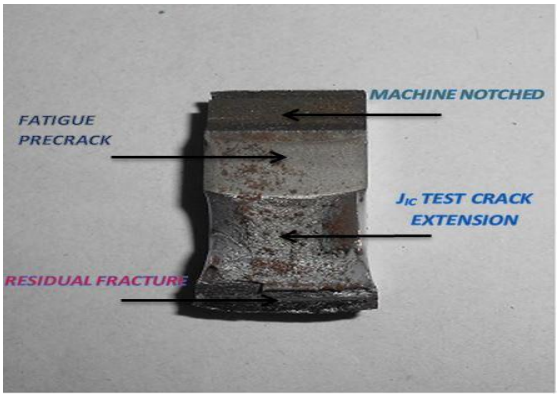

Fig. 5.15: Photograph of J_{IC} test specimen failed after testing in air

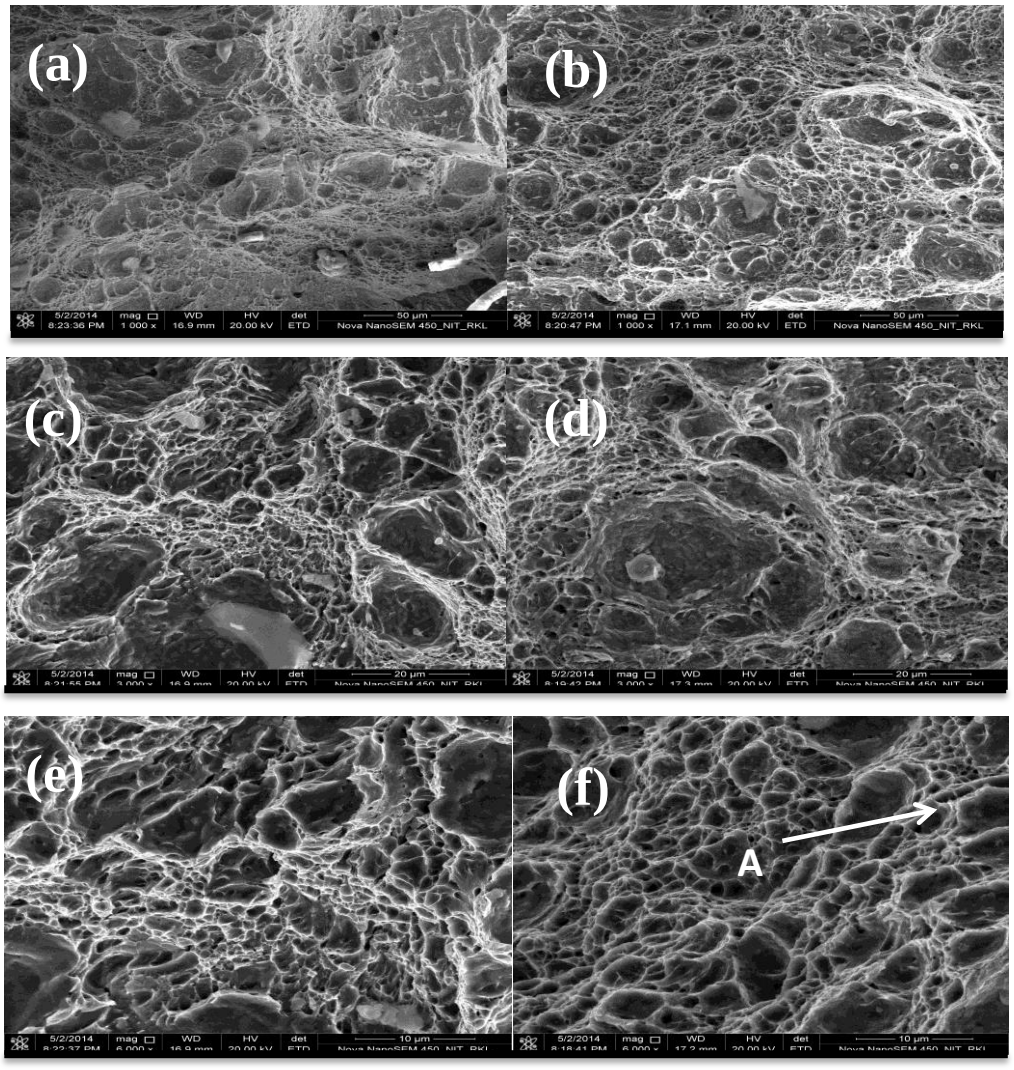

Fig. 5.16: SEM image showing the J_{IC} fracture surface in air and hydrogen in different magnification; (a),(c),(e) in air and (b),(d),(f) in hydrogen environment(A: Trans granular cleavage)

The morphology of HSLA80 shows ductile fracture in air and ductile brittle mixed fracture when charged with hydrogen. In hydrogen environment test, the decrease in ductility by hydrogen was the contributing factor of change in fracture mode**.** In sample tested in air the growth of crack is in the ductile mode with micro voids coalescence and quasi cleavage and intergranular fracture. But, for sample tested in hydrogen environment it was Trans granular in nature with minor presence of cleavage and quasi cleavage. It was also observed that the cleavage area is more in hydrogen environment compared to air tested sample.factographic feature are mostly similar in both cases.

5.4Conclusion

From the fracture tests it was observed that the HSLA80 steel has lower fracture resistance in hydrogen environment compared to air with stable crack extension. Incorporate the order of different toughness value due to hydrogen interaction.

CHAPTER6

COMPARISONS OF J_{IC} AND CTOD RESULT BETWEEN AIR AND HYDROGEN ENVIRONMENT

CHAPTER 6

COMPARISONS OF J_{IC} AND CTOD RESULT BETWEEN AIR AND HYDROGEN ENVIRONMENT

6.1 J_{IC} comparisons

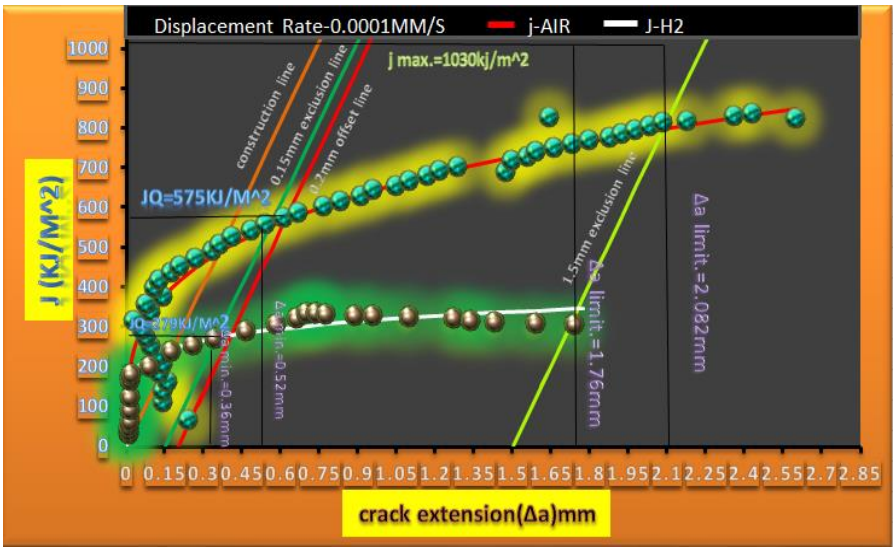

Fig. 6.1: J_{IC} comparison between air and hydrogen environment of HSLA80 sample

After analysis of mono-J test data in air and hydrogen environment it was observed fracture toughness is more in air. After validity criteria checked according to ASTM 1820-11 the J_{IC} value is 575 KJ/m^2 in air and 279KJ/m^2in hydrogen. Fig. 6.1 shows blunting line in air tested sample is elastically open widely and purely increasing in nature indicating ductile mode and large amount of plastic deformation was taken place before failure. In case of hydrogen environment very low plastic deformation and very low energy absorption was observed before failure. The graph blunting line shows reduced in ductility.

6.2 CTOD comparisons

Fig. 6.2 shows CTOD vs Δa plot for the tests carried out in both the environments. In the Fig. it can be observed that blunting line of test in air is δ_{IC} =0.442mm and in hydrogen environment is δ_{IC}=0.023mm. In hydrogen environment the crack tip elastically opens faster due to decrease in cohesive strength and quickly plastic deformation started. Crack tip

opening shown in air sample is ductile fracture in nature and hydrogen sample is less ductile-more brittle mode of failure.

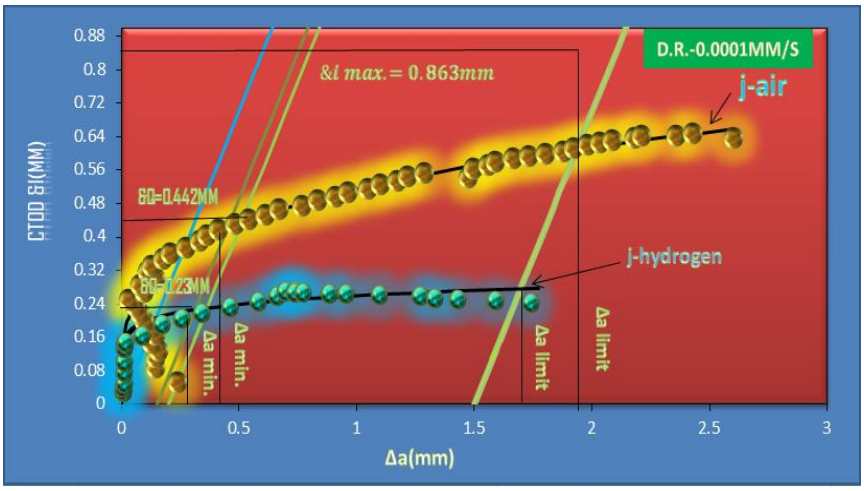

Fig. 6.2: CTOD comparisons between air and hydrogen environment tested sample

Table 6.1 shows the summery result of the both the tests and from this idea of fracture toughness of HSLA80 in both the atmosphere were obtained. This may be helpful in future use and application of the steel in this type of conditions.

Table6.1: J_{IC} and CTOD result in two different environments

	Displacement rate	current (mA/cm^2)	J_{IC} (KJ/m^2)	δ_{IC} (mm)	$\triangle a_{min.}$ (mm)	$\triangle a_{limit}$ (mm)	$P_{max.}$ (-ve) (KN)
Air	10^{-4}mm/s	-	575	0.442	0.52	2.082	-26.200
Hydrogen	10^{-4}mm/s	0.5	279	0.23	0.36	1.76	-24.322

- Since j integral apply for elastic and for completely plastic condition K_{JC} is related to J_{IC} by following relationship; $K_{JC} = \sqrt{\frac{J_{IC}E}{(1-V^2)}}$
- **Tearing modulus-** $T_{app} = \frac{E}{\sigma^2_{YS}} \frac{dj}{da}$ **and** $T_R = \frac{E}{\sigma^2_{YS}} \frac{dj_R}{da}$
- Where dJ/da= driving tearing force,

  d_{JR}/da = is the material tearing resistance which is determine from the J–R curve of the material.

  Fracture stability point for air k_{Jc}=359.24 MPa√m

  Fracture stability point for Hydrogen k_{Jc}=250.23Mpa√m

  Tearing modulus-J_{RC}=374kJ/m^2(air), 198.9kJ/m^2(hydrogen)

  The conditions for fracture instability is Tapp = TR and Japp = JR. This corresponds the intersection points in the JR–TR curve and Japp–Tapp curve. The point where intersection occurs determines the J_{Rc} value and the instability point of ductile crack growth as shown in Fig. 6.3. An applied tearing force curve (Japp–Tapp curve), a material tearing resistance curve (JR–TR curve), and their intersection point where J_{RC} is defined.

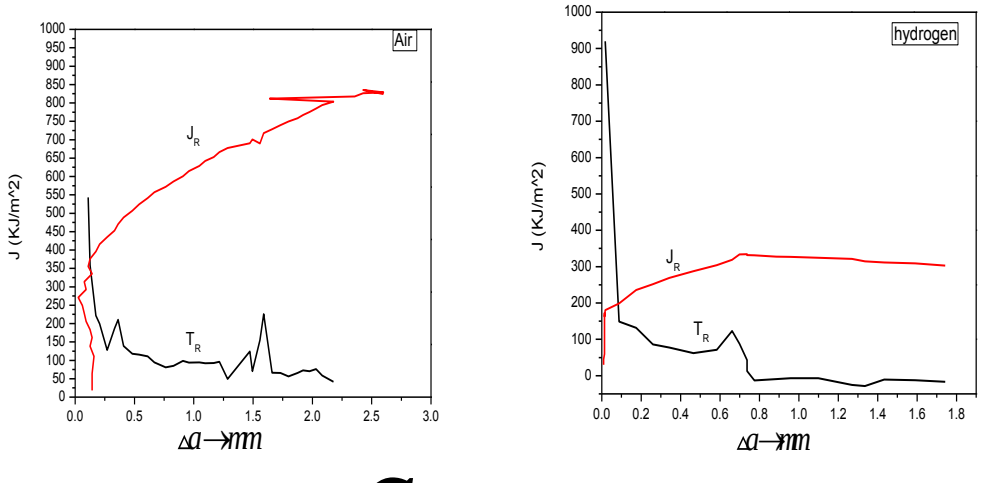

Fig. 6.3: Tearing modulus curve for HSLA80 sample tested in air and hydrogen environment

CHAPTER 7

SUMMARY AND CONCLUSIONS

CHAPTER 7

SUMMARY AND CONCLUSIONS

In the present study the J-integral and CTOD method were used in entire ductile brittle transition region to measure the elastic plastic fracture toughness. Tested HSLA80 sample is more susceptibility in hydrogen environment with compared to air with use of slow displacement rate test 0.0001mm/s. The loss of ductility is more in hydrogen environment. Following are the detailed conclusion obtained from the study:

- By microscopic study it was observed that present steel in quenched and tempered condition contains acicular ferrite, lath martensite and bainite.
- In case of fracture toughness test conducted in air the energy absorbed was 575KJ/m^2 and in case of hydrogen 279KJ/m^2 before fracture. Blunting line is more open for embrittlement test in air compared to hydrogen environment. CTOD also represents the crack tip opening of air tested sample in ductile mode and hydrogen tested sample brittle mode.
- Fracture toughness parameter J, CTOD result shows large plastic deformation occurs before failure in normal air environment sample and small plastic deformation in hydrogen tested sample.
- The Fractographic study shows similar pattern in both type of samples, in air and in hydrogen. But, in case of hydrogen environment tested sample fracture mode is slightly brittle in nature.

CHAPTER 8

REFRENCES

CHAPTER 8

REFRENCES

[1] PFEIL, L.B.; Proc.Roy.Soc.A 112(1926)182.

[2] By Richard P. Gangloff, "Hydrogen Assisted Cracking of High Strength Alloys" School of Engineering and Applied Science University of Virginia 22904-4252. 4/1/03.page6.

[3] By Gergoe.E.Dieter, brittle Hydrogen Assisted Cracking of High Strength Alloys4/1/03 Page 7 of 194.fracture and impact testing, chapter14, page no.-490.

[4] J. Ćwiek, High strength weldable steels, Mechanical Review, 9 (1996) 9-15 (in Polish).

[5] L. Coudreuse, C. Renaudin, P. Bocquet, L. Cadiou, Evaluation Of hydrogen assisted cracking resistance of high strength jackup Steels, Marine Structures 10 (1997) 85-106.

[6] Offshore Technology Report – OTO 1999 056, A review of the effects of microstructure on the hydrogen embrittlement of high strength offshore steels. Health and Safety Executive, 1999.

[7] R.A. Oriani, J.P. Hirth and M. Smialowski (eds.) Hydrogen degradation of ferrous alloys, Noyes Publ. Park, Ridge, USA, 1985.

[8] Richard P. Gangloff Department of Materials Science and Engineering School of Engineering and Applied Science University of Virginia .

[9] C.I. Garcia and A.J. DeArdo: Micro alloyed HSLA steels, Proc. World Materials Congress, Chicago, Illinois, September 24-30, 1988, p.291.

[10] M. Korchynsky (ed.): Proc. Intl. Symp. Micoalloying '75, Union Carbide Corp., New York, 1977.

[11] K.J. Irvine and F.B. Pickering: Journal of Iron Steel Institute, 1983, Vol.201, p.944.

[12] R.J. Jesseman and G.C. Schmid: Welding Journal Research Supplement, 1983, Vol.62, No.11, p.321.

[13] L.G. Kvidahl: Welding Journal, 1985, Vol.64, No.7, p.42.

[14] M Mujahid, A.K. Lis, C.I. Garcia and A.J. DeArdo: Key Engineering Materials, 1993, Vol.84-85, p.209.

[15] S.W. Poole: Properties and Selection - Iron and Steel, Metals Handbook, 10t edition, ASM, Metals Park, OH, 1973, Vol.1, p.403 .

[16] Y. Okamura, M. Okushima, H. Tamashiro, T. Kasuya, M. Tanaka, R. Yamaba, H. Inoue and A. Seto: Nippon Steel Technical Report, 1995, Vol.66, p.65.

[17] T. Zaizen, M. Sato, T. Watanabe, T. Haze, K. Okamoto, Y. Ohno and T. Kanaya: Nippon Steel Technical Report, 1983, Vol.22, p.61.

[18] I. Suzuki and Y. Hisamatsu: Journal of Electrochemical. Society, 1984, Vol.10, p.2210.

[19] B.A. Graville: Cold Cracking in Welds in HSLA Steels, ASM, Metals Park, OH, 1978, p.85.

[20] E.C. Hamre and A.M. Gilroy-Scott: Proc. Intl. Symp. Microalloying'75, Washington DC, October 1-3, 1975, p.375.

[21] J.M. Gray: Microalloyed HSLA steels, World Materials Congress, Chicago, Illinois, September 24-30, 1988, p.61.

[22] T. Gladman: The Physical Metallurgy of Microalloyed Steels, Institute of Materials, London, 1997, p.38.

[23] R. Hammer and R.W. Simon: HSLA Steels, Technology and Applications, Proc. Intl. Conf., Philadelphia, ASM, 1983, p.359 .

[24] W. Roberts: HSLA Steels, Technology and Applications, Proc. Intl. Conf., Philadelphia, ASM, 1983, p.33.

[25] C.I. Garcia, M. Mujahid, A.J. DeArdo: Proc. Intl. Conf. on High Performance Steels for Structural application, Cleveland, Ohio, 1995, p.135.

[26] F. Fukuda, T. Hashimoto and K. Kunishige: Microalloying'75, Proc. Intl. Symp., Washington DC, October 1-3, 1975, p.136 .

[27] K.J. Irvine: Steel Strengthening Mechanisms, Climax Molybdenum, Zurich, 1969, p.55.

[28] E.C. Hamre and A.M. Gilroy-Scott: Proc. Intl. Symp. Microalloying'75, Washington DC, October 1-3, 1975, p.375.

[29] Y. Okamura, M. Okushima, H. Tamechiro, T. Kasuya, M. Tanaka, R. Yamaba, H. Inoue and A. Seto: Nippon Steel Technical Report, 1995, Vol.66, p.65.

[30] W.B. Morrison: Scandinavian Journal of Metallurgy, 1980, Vol.9, p.83.

[31] C.H. Lorig and R.R. Adans: “Copper as an alloying element in steel and cast iron”, McGraw-Hill Book Co., New York, 1948.

[32] E. Hornbogen and R.C. Glenn: Transaction of Metallurgical Society, AIME, 1960, Vol.218, p.1064.

[33] E.J. Czyryca: Advances in Low Carbon High Strength Ferrous Alloys, Proc. Intl. Conf., Trans Tech Publication, Switzerland, 1993, p.491.

[34] M. Mujahid, A.K. Lis, C.I. Garcia, A.J. DeArdo and R.S. Gilbert: Fundamentals of Ageing and Tempering in Bainite and Martensite Steel Products, Proc. Intl. Symp. Montreal, Quebec, Canada, October 25-28, 1992, p.345.

[35] T. Imao, O. Chiaki, T. Tomo and S. Hiroshi: Thermomechanical Processing of High Strength Low Alloy Steels, Butterworths, 1988, p.1.

[36] E.J. Czyryca: Advances in Low Carbon High Strength Ferrous Alloys, Proc. Intl. Conf., Trans Tech Publication, Switzerland, 1993, p.491.

[37] I. Kozasu: Accelerated cooling of Steel, Proc. Intl. Conf., TMS-AIME, Pittsburg, PA, 1985, p.15.

[38] V.J. Pogorzhelskyj, Y.J. Matrosov and A.G. Nashilov: Microalloying’75, Proc. Intl. Symp., Washington DC, October 1-3, 1975, p.100.

[39] F.B. Pickering: Physical Metallurgy of Steels, McGraw Hill, New York, 1981.

[40] A. Massip and L. Meyer: Stahlund Eisen, 1978, Vol.98, p.983.

[41] E.O. Hall: Proceedings of Physical. Society of London, 1951, Vol.648, p.747.

[42] N.J. Petch: Journal of Iron and Steel Institute, 1953, Vol.25, p.174.

[43] R. Priestner and De Los Rios: Heat treatment’76, Metals Society, 1976, p.129.

[44] M. Cohen and W.S. Owen: Microalloying’75, Proc. Intl. Symp., Washington DC, October 1-3, 1975, p.2 .

[45] W.C. Leslie: Metallurgical Transaction A, 1972, Vol.3, p.5.

[46] F.B. Pickering: High strength low alloy steels – A decade of progress, Proc. Intl. Symp. Microalloying'75, Washington DC, October 1-3, 1975, p.9.

[47] F. Heisterkamp and L. Meyer: Thyssen Technical Report, 1971, Vol.1&2, p.55.

[48] G.A. Roberts and R.F. Mehl: Transaction of. American Society for Metals, 1943, Vol.31, p.613.

[49] H.I. Aaroson and H.A. Domain: Transaction of AMIE, 1966, Vol.236, p.781.

[50] F.B. Pickering: HSLA Steels Technology and Applications, Proc. Intl. Conf., Philadelphia, American Society for Metals, 1983, p.1.

[51] H.D.K.H. Bhadeshia: Bainite in Steels, Transformation Microstructure and Properties, the Institute of Materials, London, 1992.

[52] P.C.M. Rodrigues et al.Materials Science and Engineering A283 (2000) 136–143.

[53] H.K. Birnbaum, "Hydrogen Embrittlement", Encyclopedia of Materials Science and Engineering, M.B. Bever, Editor, Pergamon Press, 2240 (1986).

[54] I.M. Bernstein and A.W. Thompson, "Hydrogen Embrittlement of Steels", Encyclopedia of Materials Science and Engineering, M.B. Bever, Editor, Pergamon Press, 2241 (1988).

[55]. Bernstein, IM and Thompson, AW Hydrogen Effects in Metals, AIME, 1980.

[56].V. Raghavan Physical Metallurgy Second Edition Chapter6 "corrosion and its prevention "page no.181.

[57] J. Ćwiek, A. Zieliński Faculty of Mechanical Engineering, Gdańsk University of Technology, ul. Narutowicza 11/12, 80-952 Gdańsk, Poland, Volume 18 Issue 1-2 September–October 2006.

[58] T.L.ANDERSON chapter7"Fracture Toughness testing of metals" page no.365.

[59] Anderson, T. L., Fracture Mechanics, Fundamental and Applications, 2nd ed., CRC Press LLC, Boca Raton, Florida, 1995, pg. 4-5.

[60] ASTM, Standard test method for measurement of fracture toughness, E1820-01, ASTM, Baltimore.

[61].2005T.L. Anderson, Fracture Mechanics: Fundamentals and Applications, 1st ed. (CRC Press, 1991) p.425.

[62].Ernest J. Czyryca Development of Low-Carbon, Copper-Strengthened HSLA Steel Plate for Naval Ship Construction Ship Materials Engineering Department I Research &Development Report.

[63].T.Neeraj, R.shrinivasham, Ju.Le hydrogen embrittlement in ferrite steel Department of material science and engineering MIT Cambridge, 6th June 2012.